EFFECT OF PROCESS VARIABLES ON ATOMIZATION OF METALS AND ALLOYS

By

KAMINENI PITCHESWARA RAO

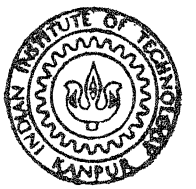

DEPARTMENT OF METALLURGICAL ENGINEERING

INDIAN INSTITUTE OF TECHNOLOGY, KANPUR

AUGUST, 1978

EFFECT OF PROCESS VARIABLES ON ATOMIZATION OF METALS AND ALLOYS

A Thesis Submitted
in Partial Fulfilment of the Requirements
for the Degree of
MASTER OF TECHNOLOGY

By
KAMINENI PITCHESWARA RAO

to the
DEPARTMENT OF METALLURGICAL ENGINEERING
INDIAN INSTITUTE OF TECHNOLOGY, KANPUR
AUGUST, 1978

ME-1978-M-RAO-EFF

DEDICATED

TO

MY BELOVED BROTHER

LATE KAMINENI RAMA KRISHNA PRASAD

(PEDDA BABU)

CERTIFICATE

This is to certify that the thesis entitled "Effect of Process Variables on Atomization of Metals and Alloys" by Mr. Kamineni Pitcheswara Rao is a record of the work carried out under my supervision and has not been submitted elsewhere for a degree.

Dr. S.P. MEHROTRA
Assistant Professor
Department of Metallurgical Engineering
Indian Institute of Technology Kanpur

ACKNOWLEDGEMENTS

I wish to express my ineffable gratitude to Dr. S.P. Mehrotra for the precious guidance, invaluable encouragement and timely suggestions given throughout the course of work.

I am very thankful to Mr. R.V. Chalam, Mr. E.S. Reddy and to my friends for their help during the work.

Thanks are also due to Mr. S.C.D. Arora for his cooperation , Mr. J.D. Varma for his elegant typing and Mr. D.K. Mishra for drawing the sketches.

Kamineni Pitcheswara Rao

TABLE OF CONTENTS

LIST OF TABLES

LIST OF FIGURES

NOMENCLATURE

$\overline{A}$, $\overline{B}$, $\overline{C}$	Constants used in Eq. (4.6)
A', B', C'	Constants used in Eq. (4.13)
b	Dimension of the long axis of oblate
B_1	Constant
C_D	Drag coefficient
d	Drop diameter = 2 r = $\overline{X}$
$\overline{d}$	Mean diameter
$\overline{d}_m$	Mass median diameter
d_{max}	Maximum drop diameter = X_m
d_M	Diameter of metal particle
$\overline{d}_{Sauter}$	Sauter mean diameter
$\overline{d}_W$	Diameter of water particle
D	Orifice or jet diameter = 2 R
D_L	Ligament diameter = 2 R_L
E	Dimensionless configuration factor
F	Dimensionless quantity
g	Gravitational constant
G_g	Mass velocity of gas or air at the nozzle outlet
G_l	Mass velocity of liquid
h	Sheet thickness
K_1	Constant in Lubanska's equation, Eq. (2.7)
K_D	Parameter in the proposed equation, Eq. (4.10)

L	Dimensionless group in Eq. (2.30)
L_b	Breakup length
L_L	Ligament length
L_W	Diameter of wetted periphery between air and liquid
m	Parameter, in Eq. (2.5)
M	Mach number
M_{fuel}	Mass flow rate of fuel lb/sec.
M_g	Mass flow rate of gas or air
M_l	Mass flow rate of liquid
M_M	Momentum of metal particle
M_W	Momentum of water particle
n	Number of metal drops, in Eq. (2.33a)
n_f	Numerical fraction of droplets
N	Number of drops, in Eq. (2.5)
$\bar{N}$	Dimensionless group, in Eq. (2.30)
P_{fuel}	Fuel pressure in lb/sq. in.
P_W	Pressure of water in KN/sq. m
Q_g	Volumetric flow rate of gas or air
Q_l	Volumetric flow rate of liquids
r_2	Radius of the constriction caused in the liquid jet
Re	Reynolds number
S.M.D	Surface mean diameter
t	Life period of ligament
U	Mean relative air wave velocity

U_S	Velocity of sound
v_d	Volume of droplet
V	Relative velocity
V_e	Velocity of expansion of the drop
V_g	Velocity of gas at impingement point
V_l	Velocity of liquid or metal
V_o	Critical velocity
V_M	Velocity of the metal particle
V_w	Velocity of water particle
W_e	Weber number
W_i	Weight of powder, defined in Eq. (4.1)
X	Distance in x - direction
X_o	Minimum droplet diameter
X_i	Mesh size, in Table 4.1
$\bar{X}_i$	Average mesh size, in Eq. (4.1)
X', y'	Parameters, defined in Eq. (4.13)
α	Amplitude of the wave
α_o	Initial value of
β	Sheltering parameter
γ	Surface tension of the liquid
ϵ	Parameter, in Eq. (2.28)
ξ_{max}	Wave number of rapidly growing wave or disturbance
θ	Atomizing angle
$\bar{\theta}$	Contact angle
λ	Wave length

μ_g	Viscosity of gas or air
μ_l	Viscosity of liquid or metal
ν_g	Kinematic viscosity of gas
ν_l	Kinematic viscosity of liquid or metal
Φ	Dimensionless group, in Eq. (2.30)
ρ_g	Density of gas or air
ρ_{go}	Density of gas or air at 300 ^{o}F
ρ_l , ρ_M	Density of liquid or metal
σ	Dimensionless rate of growth
σ_m	Standard deviation, mass basis

ABSTRACT

In the present investigation the effects of nozzle diameter, atomizing angle, temperature, and material on the atomization behaviour of molten metals and alloys have been studied. Atomization of these materials was carried out using nozzles of three different diameters (0.236 cm, 0.183 cm, and 0.1295 cm), and three different atomizers (15°, 25°, and 35°) at different temperatures. Powders were then subjected to sieve analysis. It has been found that the size distribution of powders follows a log-normal distribution pattern.

Models of Bradley and Lubanska were tested on experimental data and it was found that none of these fitted with the data in their proposed form. Modifications in these models have been proposed and it has been found that the following correlation fits in well with the experimental data.

$$\frac{\bar{d}_m}{D} = K_D \left[\left(1 + \frac{M_l}{M_g}\right) \frac{\nu_l}{\nu_g} We \right]^{m_\theta}$$

In this correlation K_D is found to be a function of nozzle diameter whereas m_θ depends on atomizing angle. The effects of nozzle diameter, atomizing angle, and temperature have been quantitatively analysed using the above correlation.

CHAPTER 1

INTRODUCTION

Atomization is a process in which a liquid stream is disintegrated into a large number of droplets of various sizes by impingement of a high velocity fluid stream. It is an interesting and important process which finds wide applications in such diverse fields as fuel injection in I.C. Engines, liquid spray drying, liquid dispersion in numerous liquid gas contact operations such as distillation, humidification, and spray crystallization etc.. Comparatively recently there has been an interest in the atomization of molten metals in connection with the production of metal powders. The essential difference between metal atomization and the atomization of other liquids is that in the former the end product always consists of solid particles. The disintegration of a stream of molten metal is carried out by using a high pressure jet fluid like air, nitrogen, argon, steam or water. The fine droplets on freezing constitute the metal powder.

In processes involving atomization the characteristics of the sprays such as average drop size, drop size distribution and spatial distribution of spray droplets of atomized liquids are of importance for reasons related to control and production efficiency in various

fields. These characteristics, in turn, depend on large number of parameters, such as physical properties of the liquid to be atomized and the atomizing media, operating variables like temperature of the liquid, liquid feed rate, pressure and feed rate of atomizing media, flight path of the droplets and quenching media (in case of production of metal powders), and design parameters e.g. nozzle design, and diameter and design of the atomizer which in turn determines the jet geometry. All these parameters and variables do individually affect the process. For an effective and meaningful control of the process it is essential that the effect of each of these parameters and variables on the process be quantitatively known. Large number of parameters and variables involved in the process makes the experimental approach of predicting the effects of these variables under various operating conditions, varying designs of atomizers and for different systems unfeasible for application because of the very large number of experiments required for such predictions. A better approach is the approach of mathematical modelling and simulation in which the effect of these parameters and variables are quantified without performing too many experiments.

Although number of studies on mathematical modelling of atomization of fluids and oils are available in literature, not much is known on the subject of molten

metals. Amongst the investigators who have dealt with the subject of mathematical modelling of molten metals, the names of Bradley[1], Lubanska[2] and others[3,4,5] can be mentioned. Their models are, however, preliminary in nature and lack generality.

The present investigation constitutes a part of a major problem, namely, the development of generalized model of atomization of molten streams which is to be taken up shortly. In this study the effect of some of the important operating variables, viz. nozzle diameter, atomizing angle, temperature on the atomization behaviour has been studied experimentally. The data thus obtained has been analyzed quantitatively with the help of some of the already existing models and thus, examining the validity of the models for the given set of operating conditions. Wherever possible modifications in the models have been proposed for better prediction of results.

CHAPTER 2

LITERATURE REVIEW

In literature, the effects of operating variables on atomization of liquid streams have been discussed both qualitatively as well as quantitatively. A thorough review of the literature on the qualitative discussion of these effects has been presented by Khedar in his Master's dissertation[6]. To avoid repetition, in this chapter, we have only tried to review the literature on quantitative aspects of atomization studies. As it has been pointed out in the previous chapter also the present investigation constitutes only a part of the ultimate objective, namely, the development of a generalized mathematical model for atomization of molten metals under varying operating conditions. Only with this ultimate objective in mind the literature has been reviewed and presented in this chapter.

For convenience the quantitative models that could be reviewed have been grouped in three categories:

i) emperical-semiemperical models,

ii) mathematical models based on analytical approach, and iii) statistical models.

Under first category of models come those in which various correlations have been established using dimensionless

numbers or variables. The values of various constants involved in these correlations have been obtained emperically using mostly curve fitting methods. The main drawback of these models is that they are applicable only for those sets of operating conditions for which the correlations have been established.

In the case of analytical models the model equations are derived from the first principles. Here the model equations are more rigorous and complex in nature and in some cases, may even be difficult to solve. However, they provide an insight to the actual physical phenomenon and should be applicable to a much wider range of operating conditions, if the boundary conditions are properly chosen.

As the heading suggests, the statistical models are based on statistical approach. However, not many models based on this approach are available in literature. This approach would be useful only if a very large set of data is available.

The above classification is by no means very rigorous. Some overlapping is unavoidable and in some cases it is possible to classify a model in one group or the other.

2.1 EMPERICAL-SEMIEMPERICAL MODELS

Nukiyama and Tanasawa[7] proposed a correlation in late thirties relating Sauter mean drop diameter to the gas and liquid flow rates and liquid properties for two fluid atomization.

$$\bar{d}_{Sauter} = \frac{585}{V}\sqrt{\frac{\gamma}{\rho_l}} + 597\left(\frac{\mu_l}{\gamma\rho_l}\right)^{0.45}\left(1000\,\frac{Q_l}{Q_g}\right)^{1.5} \qquad (2.1)$$

where $\bar{d}_{Sauter}$ is Sauter mean diameter*, V is relative velocity, γ, ρ_l and μ_l are surface tension, density and viscosity of liquid respectively, and Q_l and Q_g are the feed rate (volumetric) of liquid and air respectively. For inviscid liquids at flow rates of $Q_g/Q_l > 5000$ the contribution from the second term is negligible and the relative velocity reaches sonic velocity for most nozzles at this ratio of Q_g and Q_l. Now $\bar{d}_{Sauter}$ is clearly related to the well known dimensionless Weber number, which represents the

---

* Sauter mean diameter is defined by the relation[8]

$$\bar{d}_{Sauter}\int_{X_o}^{X_m}\bar{X}^2\,\frac{d\,n_f}{d\,\bar{x}}\,d\,\bar{x} = \int_{X_o}^{X_m}\bar{X}^3\,\frac{d\,n_f}{d\,\bar{x}}\,d\,\bar{x}$$

where $\bar{X}$ is drop diameter, X_o is minimum droplet diameter, X_m is maximum droplet diameter, n_f is numerical fraction of droplets having diameters $< \bar{X}$.

ratio of inertial forces to the interfacial forces in studies of liquid break-up phenomena. So the value of the predicted drop sizes approaches a constant which primarily depends on liquid density and surface tension.

Ohnesorge[9] found a critical velocity V_o below which, according to him, the drop size reaches a constant value and uniform size which is dependent on nozzle diameter. The critical velocity, V_o, could be evaluated from the following emperical relationship

$$\frac{\mu_l}{\sqrt{\rho_l \sigma D}} = 2000 \left(\frac{\mu_l}{V_o \rho_l D} \right)^{4/3} \qquad (2.2)$$

where D is nozzle diameter. Eq. (2.2), however, does not seem to be valid for two fluid atomization (where liquid stream is hit up by high velocity fluid), where the mean drop size is not constant even at low velocities.

A completely emperical model for predicting mean size of drops for one fluid atomization is given by Merrington and Richardson[10], in which, the break up of the jet is assumed to be completely controlled by viscous and inertial forces at speeds higher than the critical velocity V_o given by Eq. (2.2). At these speeds Schewitzer theory* is assumed to be valid, viz, atomization can not be

---

* Cited by Merrington and Richardson[10]

achieved without air friction, and to make air friction effective, turbulence within the jet is essential. The emperical relationship between the velocity and the droplet size as obtained by these authors[10] is

$$\frac{V\,\bar{d}}{\nu_l^{1/5}} = 500 \qquad (2.3)$$

where $\bar{d}$ is mean size and ν_l is kinematic viscosity. This equation seems to suffer from two main drawbacks, firstly, it appears to be dimensionally unsound, and secondly, it does not take into account the surface tensional effects and, therefore, does not seem to be valid for the conditions beyond the experimental range.

A correlation applicable for swirl atomization (atomization taking place in I.C. Engines) has been proposed by Clare and Radcliffe[11].

$$S.M.D. = 182 \frac{M_{fuel}^{0.25}}{P_{fuel}^{0.4}} \qquad (2.4)$$

where S.M.D. is surface mean diameter, M_{fuel} is fuel flow rate in lb/hr and P_{fuel} is fuel pressure in lb/sq. in. . As M_{fuel} is very nearly proportional to the square of the atomizer dimensions, the diameter of the droplet produced by swirl atomizers at constant pressure seems to be proportional to the square root of the orifice diameter.

Clare and Radcliffe measured the droplet distribution for such an atomizer using wax simulation technique and found the following differential equation to be valid.

$$d(N) = m N e^{-md} d(d) \qquad (2.5)$$

where N is number of drops, m is a parameter and d is droplet diameter. The equation is valid for air/fuel ratio $\simeq 0.1$ and the viscosity values ranging from 20 to 40 cp, above which swirl atomizer can not be used for atomization at all. As the fuel pressure increases, the drop size decreases at constant air/fuel ratio possibly because the fuel velocity is sufficiently high to cause atomization. Both Eqs. (2.4) and (2.5) are not applicable, in general, for common atomization processes where relative velocity is an important parameter.

Depending on the results of Clare and Radcliffe[11] and using dimensional analysis, Wigg[12] arrived at an equation

$$\bar{d}_m = \frac{200 \times 10^3 \nu_l^{0.5} M_l^{0.1} (1 + \frac{M_l}{M_g})^{1/2} D^{0.1} \gamma^{0.2}}{\rho_g^{0.3} V_g} \qquad (2.6)$$

where V_g is velocity of gas at impingement with the stream, and M_l and M_g are mass flow rates of liquid and gas, respectively. This equation has been found to be applicable only for certain types of liquids, eg. wax.

Lubanska[2] modified the above equation for fitting his experimental data obtained using spray ring atomizer with tin, iron, and low melting alloys and arrived at the following equation

$$\frac{\bar{d}_m}{D} = K_1 \left[\left(1 + \frac{M_l}{M_g}\right) \frac{\nu_l}{\nu_g \cdot We} \right]^{1/2} \qquad (2.7)$$

where 'We' is dimensionless Weber number and ν_g, in fact a constant, is kinematic viscosity of gas. Experimental data of Tamura[13], Thompson[14], and Clare[11] seem to fit with Eq. (2.7). The value of K_1 is chosen for particular conditions of spray ring and liquid stream and in most cases vary between 40 and 50.

Weiss and Worsham[15] made an experimental study of drop sizes obtained on injecting a liquid into a large hot air stream of sustained velocity and proposed the following correlation

$$\bar{d}_m \propto V^{-1.33} \; G_l^{0.08} \; D^{0.16} \; \mu_l^{0.34} \left(1 + \frac{\rho_{g\,o}}{\rho_g}\right) \qquad (2.8)$$

where G_l is mass velocity of liquid and $\rho_{g\,o}$ is density of air at 300°F. This equation does not take into account the effect of surface tension, viscosity of air, and density of liquid. When these effects were incorporated using dimensional analysis, the above Eq. (2.8) was modified to

$$\frac{\bar{d}_m \rho_g V^2}{\sigma} = 0.61 \left(\frac{V\mu_l}{\sigma} \right)^{2/3} \left(1 + \frac{10^3 \rho_g}{\rho_l}\right) \left(\frac{N_l \rho_l \sigma \mu_g}{\mu_l^4} \right)^{1/12} \quad (2.9)$$

where ρ_g is density of air at the temperature of atomization and μ_g is viscosity of air. The effect of geometry of injectors is negligible especially at high velocities. The Eq. (2.9) agrees well with the Weiss and Worsham experimental data which was obtained for large relative velocities (100 to 1000 ft/sec.). The standard deviation is only 12 percent for data which has We $\left(\frac{\bar{d}_m \rho_g V^2}{\sigma} \right) > 25$. The deviation seems to increase with decreasing relative velocity. The main drawbacks of this correlation are i) the equation assumes $\rho_l / \rho_{g\,o} = 10^3$ which may not be valid in many atomization processes, and ii) temperature is assumed to be constant.

Gretzinger and Marshall[16], from their experimental data, concluded that the drop size of sprays varied significantly with mass flow ratio of air to liquid and the data could be fitted with a hyperbola, only if the liquid flow rate was greater than 1 gal/min. At low flow rates the dropsizes increased because of the pulsating and unstable spray flow. They further observed that the mass median diameter at constant mass flow ratio decreased with increasing liquid flow rate. This was, according to them,

due to the fact that the liquid spread over a great exit perimeter and so the liquid film thickness was decreased. They also observed that the drop size decreased as the air orifice size was increased upto 0.125 inch at which the trend ceased. Using the experimental data they obtained following emperical equations for mean size and standard deviation as a function of liquid and air properties for two different types of nozzles. For converging pneumatic type of nozzles

$$\bar{d}_m = 2600 \left[\frac{M_l}{M_g}\right]^{0.4} \left[\frac{\mu_g}{G_g L_w}\right]^{0.4} \quad \text{and} \quad \sigma_m = 1.77\, \bar{d}_m^{0.4} \tag{2.10}$$

where σ_m is standard deviation, G_g is mass velocity of air at the nozzle outlet, and L_w is diameter of wetted periphery between air and liquid. For pneumatic impingement type of nozzles

$$\bar{d}_m = 122 \left[\frac{M_l}{M_g}\right]^{0.6} \left[\frac{\mu_g}{G_g L_w}\right]^{0.15} \quad \text{and} \quad \sigma_m = 1.735\, \bar{d}_m^{0.16} \tag{2.11}$$

As the model is emperical the usage of it to other types of atomizers and also beyond the ranges of variables studied is very doubtful. According to Gretzinger and Marshall[16] themselves, these equations are not likely to be applicable for the cases in which the streams meet at

right angles. The equations may give satisfactory results for liquids having viscosities close to 1 cp and surface tension of 50 dynes/cm. Further, the Reynolds number of flow should be < 1000 and the film thickness, calculated by using Friedman and Miller method[17], between 0.3 and 0.6 cm. These equations have been used in design of spray evaporation and drying problems.

Several other emperical correlations given by other investigators for different types of atomizers are also available in literature. Gelperin et al.[18] proposed the following equation for dispersion of caustic alkali melts in column granulators:

$$\frac{\bar{d}}{D} = 11{,}922\ Re^{-0.23}\ (\rho_g/\rho_l)^{0.73}\ (\mu_g/\mu_l)^{0.23} \qquad (2.12)$$

where Re is Reynolds number.

Rizkalla et al.[19], from their work on air blast atomizer, found

$$\bar{d}_{Sauter} = 521\ V_g^{-1}\ \sigma^{0.5}\ \rho_l^{0.75}\ (1 + \frac{M_l}{M_g}) + 0.037\ \mu_l^{0.85}\ (\sigma\rho_l)^{1.2}\ (1 + \frac{M_l}{M_g})^2 \qquad (2.13)$$

where $\bar{d}_{Sauter}$ is Sauter mean diameter. The effect of pneumatic sprayer design was studied by Fainerman et al.[20]

and the correlation obtained is

$$\frac{\bar{d}_{Sauter}}{D} = 1.27 \ We^{-0.5} \qquad (2.14)$$

2.2 ANALYTICAL MODELS

In most commonly used approach in developing analytical models, the liquid stream is visualized as a wave and the mechanism of disintegration of this stream is derived from the wave disturbance mechanism. In this approach it is assumed that the disintegration of a liquid stream takes place due to continuous increase in surface area of a rod or sheet of liquid until it becomes unstable and finally disintegrates. The threads or ligaments are torn off the slower moving liquid by the surrounding high velocity fluid stream, in case of two fluid atomization, or by the air friction in the case of one fluid atomization where ligaments are lost to still medium. These ligaments are of such sizes that they will eventually breakup into drops of the sizes observed finally in the spray. According to Plateau,[21] a cylindrical column whose length exceeds its circumference is unstable and will eventually collapse under the influence of any disturbance created by air stream or turbulence in the liquid jet itself. Disruption occurs when the depth of any disturbance in the sheet is of the size of sheet thickness. Some of the models based on this approach are discussed below.

Rayleigh[22] was amongst the first investigators who analyzed the disintegration of a jet applying the concept of small disturbance. He postulated that all the disturbances at randomly and the disturbance that grows most rapidly will cause the breakup of the jet and the resulting ligaments depend on the wave length of the disturbance which is given by

$$\lambda = 4.508 \times 2R \qquad (2.15)$$

where R is jet radius. For the collapse of the liquid ligaments the amplitude of the disturbance is given by

$$\alpha = \alpha_o e^{qt} \quad \text{or} \quad q = \left(\frac{\gamma}{\rho_l R_L^3} \right)^{1/2} F \qquad (2.16)$$

where α_o is initial value of amplitude α, t is life period of ligament, F is a dimensionless quantity and is a function of $L_L/2R_L$ where L_L is length of ligament and R_L is radius of ligament. He concluded that the disturbance which caused the breakup was the one having maximum F.

Based on the similar approach, Castleman[23] derived a mathematical expression relating R_L and the radius of the drop r as

$$R_L = \left(\frac{2}{3Z} \right)^{1/3} r \qquad (2.17)$$

where $Z = L_L/2\,R_L$. He observed that the maximum value of F in Eq. (2.16) was obtained at $Z = 4.5$. He finally arrived at

$$R_L = 0.53\ r \qquad (2.18)$$

He also calculated the life period of ligament using Eq. (2.16) which could be rewritten as

$$t = \frac{1}{q} \ln (\eta/\eta_o) \qquad (2.19)$$

According to him the ligament breaks down when amplitude grows to a value of R_L. As the air speed increases the ligament size and breakup times decrease, and the drop size reaches a constant value when the ligaments collapse as soon as they are formed. This happens at high velocities in the range of 10,000 to 12,000 cm/sec (Sauter)[24]. This velocity range is only applicable for gas atomization. From Eqs. (2.16) and (2.19) it is evident that the ligament formation and breakup would be faster even at low velocities for liquids of low surface tension.

Weber[25] simplified Rayleigh's equations, considering the distortion of the centre line of a jet by the effect of air forces. In this case, the cross section of the jet remains constant and the resultant sinuous jet was considered as an elastic beam subjected to thrust and bending. So, by modifying the classical equations of

elasticity, equations for the equilibrium of forces and moments acting on a segment of the sinuous jet, he could arrive at an expression analytically for the breakup length of the jet

$$L_b = \frac{V_l \sqrt{\rho_l R^3}}{\sigma} \log_e \left(\frac{R}{\alpha_o} \right) \qquad (2.20)$$

where L_b is breakup length and σ is dimensionless rate of growth.

Assuming that the volume of the droplets obtained from primary disintegration of the jet is equal to the volume of a cylinder with radius equal to that of the jet, R, and with length equal to the wavelength of the most rapidly growing disturbance, Tyler[26] obtained the equation for maximum diameter, d_{max} of droplets as

$$\frac{d_{max}}{2R} = \sqrt[3]{\frac{1.5\lambda}{2R}} \qquad (2.21)$$

This was the first plausible conjecture which fitted well with the experimental data closely. This correlation is unlikely to be valid for the systems where there is a turbulence in the stream which may result in secondary atomization.

Using the same approach as that given by Weiss and Worsham[15], Mayer[27] developed a semi-analytical mathematical model of atomization. According to him, because

of viscous dissipation waves of very small wave lengths and because of inertial effects waves of very large wave lengths can not be developed. Therefore only a restricted spectrum of wave lengths can be excited to appreciable amplitudes during the time of action of high velocity gas flow. The mean diameter of the droplet developed by the excitation of wave having wave length λ is given by

$$\bar{d} = E\lambda \tag{2.22}$$

where E is a dimensionless configuration factor which depends on liquid viscosity, but is independent of gas velocity, liquid density, wave length, surface tension, and gas velocity and

$$\lambda = 9\pi \sqrt{3/16} \left(\frac{\mu_l \sqrt{\sigma/\rho_l}}{\beta \cdot \rho_g V_g^2} \right)^{2/3} \tag{2.23}$$

where β is known as sheltering parameter. Substitution of Eq. (2.23) in (2.22) results in

$$\bar{d} = 9\pi \sqrt{3/16} \; B \left(\frac{\mu_l \sqrt{\sigma/\rho_l}}{\rho_g V_g^2} \right)^{2/3} \tag{2.24}$$

where $B = E/\beta^{2/3}$ is a composite numerical factor including sheltering parameter β. Comparison of the theoretical mean diameter predicted by Eq. (2.24) with that of experimental data of Weiss and Worsham[15] showed a good agreement. Mayer also suggested that the reference

temperature for correlating dropsize data with liquid properties when there is difference in temperature of gas and liquid, should be either the gas temperature or the boiling temperature of liquid whichever is smaller. The model, however, does not incorporate the effects of nozzle angle, liquid flow rate, liquid velocity and air flow rate on drop size.

Assuming the same mechanism of atomization as that assumed by Castleman and others, and considering the force balance between surface tension, pressure and inertial forces Dombrowski and Johns[28] obtained the average droplet diameter produced on disintegration of fan spray sheet as

$$d = \left(\frac{3\pi}{2}\right)^{1/3} D_L \left(1 + \frac{3\mu_l}{\rho_l \gamma D_L}\right)^{1/6} \qquad (2.25)$$

where

$$D_L = 0.9614 \left(\frac{K^2 \gamma^2}{\rho_g \rho_l U^4}\right)^{1/6} \left(1 + 2.60 \mu_l \sqrt[3]{\frac{K \rho_g^4 U^7}{72 \rho_l^2 \gamma^5}}\right)^{1/5}$$

where $K = h x$ = (sheet thickness) (distance in x - direction), U is mean relative air wave velocity as given by Dombrowski and Johns[28]. The validity of Eq. (2.25) has been tested by Bruce See et al.[29] using experimental data for disintegration of lead stream.

Holroyd[30] used the method of dimensional analysis to correlated dimensionless maximum droplet diameter,

$d_{max}/2R$ with the Weber and Reynold numbers. Assuming that the density ρ_l, the velocity V_l, the viscosity μ_l, the surface tension σ, jet radius R are the variables which affect the primary droplet formation, he obtained the following correlation

$$\frac{d_{max}}{2R} = We^{-2/3} f(Re) \qquad (2.26)$$

In this approach major emphasis is on the centrifugal forces within a liquid jet which play an important role in the process of disintegration of the jet. Although a plot of $We^{2/3} \frac{d_{max}}{2R}$ Vs Re failed to give a linear plot, substitution of $\frac{d_{max}}{2R}$ by Eq. (2.21) resulted in a remarkably linear correlation.

Miesse[31] proposed a modification in Holroyd's correlation as follows for his experimental data:

$$\frac{d_{max}}{2R} = We^{-2/3} (23.5 + 0.000395\ Re), \quad \text{or} \qquad (2.27a)$$

$$\frac{d_{max}}{2R} = \sqrt[3]{\frac{\sigma}{2\rho_l R V_l^2}} \left(23.5 + 0.000395 \frac{2\rho_l R V_l}{\mu_l}\right) \qquad (2.27b)$$

Truely speaking it is a semianalytical correlation. According to Eq. (2.27) the maximum droplet diameter increases with increase in nozzle radius, surface tension and will decrease with increase in viscosity. This

decrease in droplet diameter with increase in viscosity may be due to the fact that with increase in viscosity the spray sheet thickness decreases. Increase in velocity decreases maximum droplet diameter for $Re < 11.9 \times 10^4$ and will increase it for larger values of Reynolds number. This might be because of greater splashing at high velocities which result in large drops or flakes. The splashing may be because of the resulting large negative pressure gradient radial to the flow of liquid at high velocity. Also, increase in density of liquid will decrease the droplet diameter for $Re < 2.975 \times 10^4$ and will increase it for larger values.

Bradley[1] developed a semi-analytical model based on Castleman[23] and Rayleigh's[22] approach. Assuming that the ligament formed has diameter which is some fraction of fastest growing wave length, Bradley got

$$D_L = 2 R_L = \frac{2\pi\epsilon}{\varphi_{max}} \qquad (2.28)$$

where φ_{max} is the wave number of the fastest growing disturbance of wave, and $0 < \epsilon < 1$. Using Castleman relation (Eq. (2.18)) between drop size diameter and ligament diameter, he obtained the following relationship

$$d = \frac{11.8\,\epsilon}{\varphi_{max}} \qquad (2.29)$$

Intutively ϵ was taken as 1/4. Since σ_{max} increases with increasing air wave velocity, according to Eq. (2.29) drop size will decrease. Using dimensional analysis, Bradley investigated the effect of physical properties of the metal on drop size. Seven important variables were grouped into four dimensionless group as below.

$$L = \frac{\sigma_{max}\, \delta}{\rho_g U_s^2}, \quad \rho = \frac{\rho_g}{\rho_l}, \quad M = \frac{V}{U_s}, \quad \bar{N} = \frac{\mu}{\rho_g U_s \delta} \tag{2.30}$$

where U_s is velocity of sound and V is relative velocity. Using a graphical approach Bradley arrived at the following relationship between the drop size diameter and the properties of liquid and gas

$$2r = d = \frac{2.95\, \delta}{L\, \rho_g U_s^2} \tag{2.31}$$

Eq. (2.31) may require some modifications as it is well known that the effect of surface tension on drop size will not be as much as predicted by this equation.

The model proposed by Rajinder Kumar and Laxmi Prasad[32] to explain their data on convergent type pneumatic atonizers is quite exhaustive. According to them, liquid jet is considerably contracted by the impaction of high velocity gas and the drops are formed at this constriction and not at the nozzle trip itself. It was

assumed that the drop expands with its base attached to the constriction. This expanding drop is assumed as a moving drop, its velocity being equal to the velocity with which the center of the drop moves and also the drop itself is an oblate in shape. Various forces come into play during expansion of the drop, some of them assist detachment and others prevent detachment. At the time of detachment, the upward and downward forces are counter-balanced. Resisting forces are surface tension force (F_I), expansion force (F_{II}), drag force (F_{III}) and force due to tensile viscosity (F_{IV}). The downward forces are net drop weight (F_V), force due to kinetic energy of the liquid (F_{VI}), and force due to kinetic energy of the gas (F_{VII}).

$$\text{Therefore, } F_I + F_{II} + F_{III} + F_{IV} = F_V + F_{VI} + F_{VII} \qquad (2.32a)$$

For the droplet under consideration force balance gave

$$2\pi R \sigma \cos\bar{\theta} + \frac{Q_l^2 \rho_l v_d^{-2/3}}{14.5\left[\frac{Q_l \rho_l V_g}{2.5 \times 10^4}\right]^{2/3}} + \frac{1}{2}\rho_g V_e^2 C_D \pi b^2$$

$$+ \pi r_2^2 \mu_l Q_l v_d^{-1/6} = v_d(\rho_l - \rho_g) g + (Q_l^2 \rho_l / \pi r_2^2)$$

$$+ (Q_g \rho_g V_g) \text{ or } (Q_l \rho_l V_g) \text{ whichever is smaller} \qquad (2.32b)$$

where $\bar{\theta}$ is contact angle, v_d is volume of droplet, C_D is drag coefficient, b is long axis of oblate, and r_2 is the radius of the constriction caused in the liquid jet. When the liquid emerges into an atmosphere with normal pressure and temperature, forces due to surface tension, drag and buoyancy will not contribute to more than 1% and so can be neglected and Eq. (2.32 b) could be simplified to

$$\pi r_2^2 \mu_1 Q_1 v_d^{-1} / 6 + \frac{Q_1^2 \rho_1 v_d^{-2/3}}{14.5 \left[\frac{Q_1 \rho_1 V_g}{2.5 \times 10^4} \right]^{2/3}}$$

$$= (Q_g \rho_g V_g) \text{ or } (Q_1 \rho_1 V_g) + \left(\frac{Q_1^2 \rho_1}{\pi r_2^2} \right) \qquad (2.32c)$$

This was the final equation of the model which could be verified with experimental data. Because of fluctuations in air velocity, secondary atomization and coalescence, the droplet size distributions are obtained with considerable skew. Effects of viscosity, surface tension, air velocity as predicted by the model agreed well with the experimental data over a considerably wide range.

Most of the models suggested are for pneumatic atomization or gas atomization of liquid streams. Small and Bruce[33], Gummeson[34] and others indicate that the median size and other properties of drops formed by water

and gas atomization differ largely, so it is apparent that the work on gas atomization is not very much suitable for description of water atomization. Actually water atomization deals with dispersed particles of water striking the metal stream when compared to gas phase which is continuous. So the correlations obtained for gas atomization hardly have any use for predictions in water atomization.

An analytical model for water atomization of liquids has been developed by Grandzol and Tallmadge[3]. The model was based on (a) a momentum exchange equation for size, (b) use of literature equations of Straus[35], Fraser and Eisenklam[36], Merrington[10] for water droplet size as a function of water jet velocity, (c) a kinetic energy equation for the velocity ratio, and (d) metal particle velocity obtained by special photographic determination. The model does not specifically describe any mechanism for preliminary breakup of metal stream. Assuming that the water droplet transfers all its momentum M_W to the newly formed 'n' number of metal droplets, each of momentum M_M, a momentum balance gives

$$n \; M_M = M_W \qquad (2.33a)$$

This can be rewritten as

$$d_M = \left(\frac{V_W \rho_W}{n \; V_M \rho_M} \right)^{1/3} d_W \qquad (2.33b)$$

where V_w is water droplet velocity derived from the pressure of water by using $V_w = 1.3\ P_w^{1/2}$ where P_w is the pressure in K N / m^2, and V_M is the resultant metal particle velocity which is found by photographic technique. d_w is deduced from the correlations of Straus[35], Frazer and Eisenklam[36]. From their data

$$d_w = \frac{B_1}{V_w} \qquad (2.34)$$

where B_1 is a constant. Eq. (2.34) is similar to the one given by Merrington and Richardson[10]. Substituting the values of different variables, B_1 was found to be of the order of 20,000. Therefore

$$d_M = \left(\frac{V_w \rho_w}{n V_M \rho_M} \right)^{1/3} \left(\frac{20,000}{V_w} \right) \qquad (2.35a)$$

V_w/V_M was almost constant and was equal to 50/15.3. So,

$$d_M = \frac{14,900}{V_M} \left(\frac{1}{n} \right)^{1/3} \qquad (2.35b)$$

The effects of various nozzle sizes, jet parameters and metal flow parameters could be explained using Eq. (2.35b). The model, however, does not incorporate the effects of variation of metal properties and jet angles.

2.3 STATISTICAL MODELS

An altogether new approach based on statistical analysis has been developed by U.R. Date et al.[4] for interpreting metal atomization. The yields of different mesh fractions were taken at different operating pressures, temperatures for some atomizing nozzles. Taking pressure as the important parameter, following equations were arrived at, using regression analysis

$$Y = \bar{y} + \frac{\Sigma y Z_1}{\Sigma Z_1^2} \left(\frac{P_r - \bar{P}_r}{2} \right) \tag{2.36a}$$

$$Y = \bar{y} + \frac{\Sigma y Z_1}{\Sigma Z_1^2} \left(\frac{P_r - \bar{P}_r}{2} \right) + \frac{\Sigma y Z_2}{\Sigma Z_2^2} \left\{ \frac{(P_r - \bar{P}_r)^2}{2} - 2 \right\} \tag{2.36b}$$

where Y is the percentage yield of the particular mesh size for which the equation is developed, $\bar{P}_r$ is the average pressure of all the experiments over which the data are collected, P_r is the actual pressure in the particular experiment, which is of interest. $\bar{y}$, $\Sigma y Z_1$, ΣZ_1^2, $\Sigma y Z_2$, ΣZ_2^2 are the terms which are used in regression analysis. Eq. (2.36a) is a first order equation and Eq. (2.36b) is a second order equation. Such equations of different orders can be obtained for all size fractions for different nozzle diameters. In fact, such statistical models can be

constructed for any experimental data on atomization, taking the most important variables affecting the process of atomization. This type of models would mainly be useful to simulate the existing atomizers but of little use in new designs.

CHAPTER 3

EXPERIMENTAL

This chapter mainly deals with the description of the experimental unit and the experimental procedure.

3.1 DESCRIPTION OF EXPERIMENTAL UNIT

The same experimental set-up that was fabricated by Khedkar[6] has been used in this study after making some modifications. A schematic diagram of the experimental unit is shown in Fig. 3.1. A brief description of the unit is given below.

The main components of the atomizing unit are:

(i) melting unit with a temperature controlling device,
(ii) container to melt and hold the metal,
(iii) nozzle-atomizer assembly,
(iv) stopper rod, and
(v) water tank to quench and collect the atomized particles.

3.1.1 Melting Unit

It consists of a vertical muffle type resistance furnace with 60 cm outer diameter and 37.5 cm height having both ends open and actual working zone of 37.5 x 10 x 10 cm^3. A schematic diagram of the furnace as a

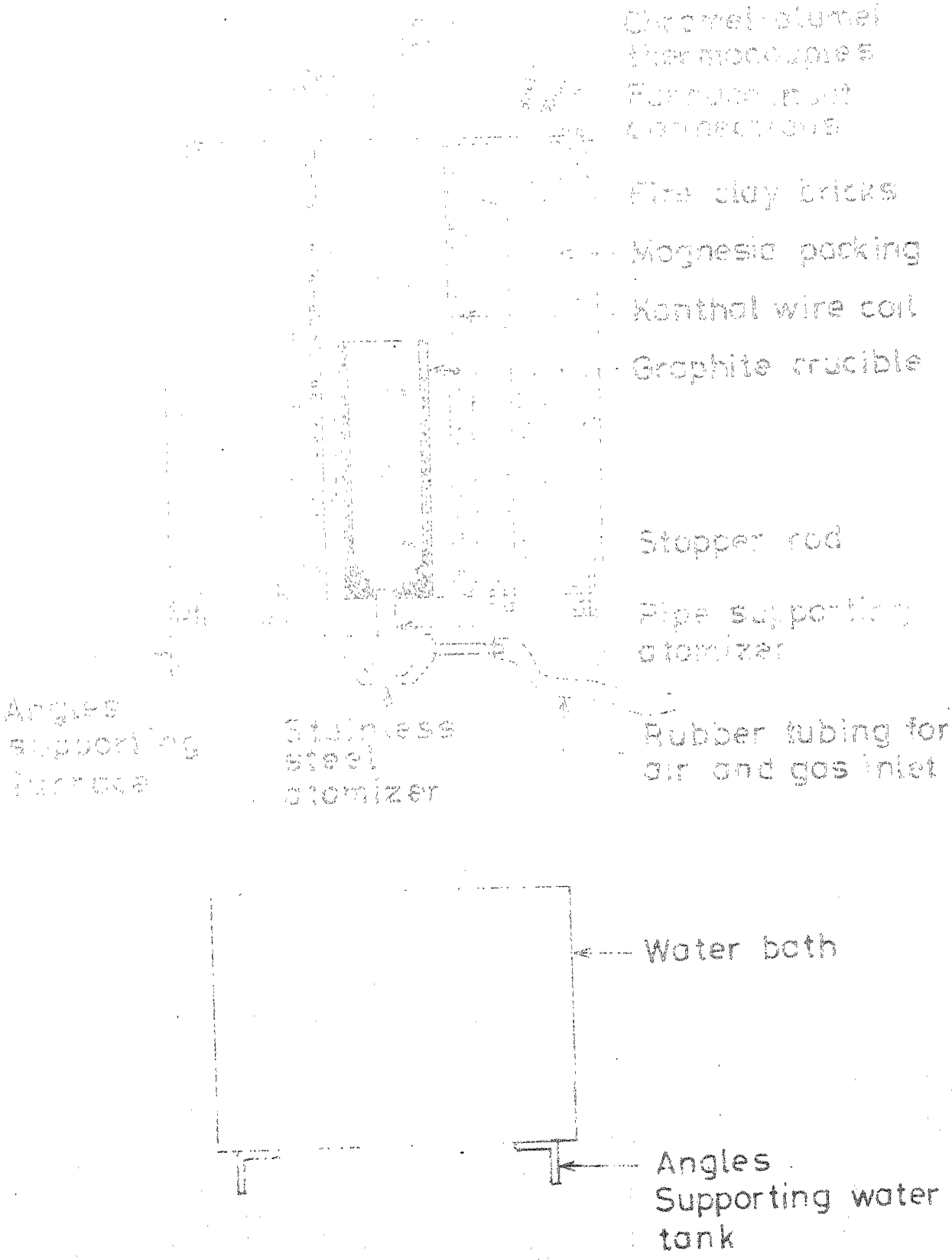

Fig 3.1 Atomization set-up[6]

part of atomizing unit is shown in Fig. 3.1. A 1/2" diameter coil of Kanthal Wire (16 gauge), embeded in vertical slots specially made in fireclay bricks, was used as the heating element in the furnace. The coil was kept half exposed to the container to attain as high temperature as possible without increasing the power input. Openings for placing two thermocouples in the centre of the furnace were provided. One of the thermocouples could be connected to a temperature controlling unit and the other to a potentiometer for direct measurement of temperature of molten metal.

3.1.2 Container

The metal to be atomized could be melt and then held in a cylindrical graphite crucible of 7.5 cm diameter and 20 cm length. A two step hole as shown in Fig. 3.2 was drilled at the bottom of the crucible. One of these steps provided the base for resting the nozzle and the other one helped in holding the steel tube whose other end was threaded to hold the atomizer. As Khedkar also observed[6], the shape of the crucible is an important factor to avoid accumulation of molten metal at the end of each atomization run.

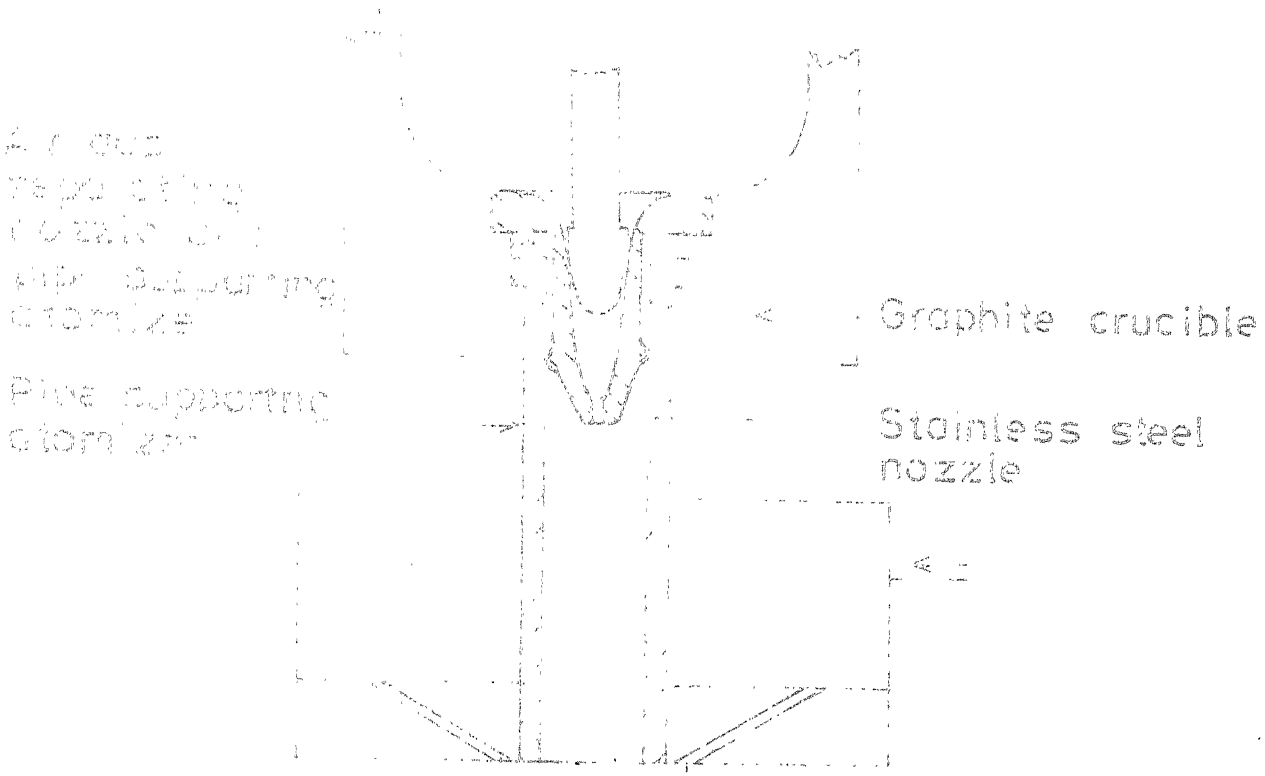

Fig. 3.2 Nozzle atomizer assembly

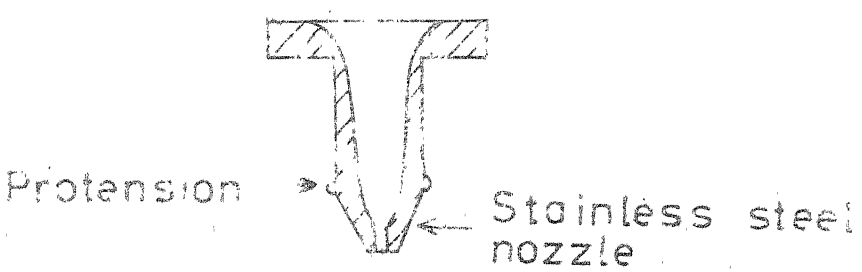

Fig. 3.3 Nozzle

3.1.3 Nozzle Atomizer Assembly

Nozzles and atomizers of various designs were tried out by Khedkar[6]. The assembly that was most successful, according to him, was used in the present investigation after making some modifications in the design of the atomizer. A brief description of the design of the nozzle and the atomizer is given below.

3.1.3.1 Nozzle: Three stainless steel nozzles with opening diameters of 0.1295 cm, 0.183 cm and 0.236 cm were fabricated. The 'V' shaped cavity of these nozzles (Fig. 3.3) provided seat for the stainless steel stopper rod. A small protension was made near the bottom of the nozzle for alignment purpose.

3.1.3.2 Atomizer: The stainless steel atomizer fabricated by Khedkar had six symmetric holes or jets of 1/8" diameter, each inclined at an angle of 45^{o} with the vertical axis and meeting at a common impingement point with the vertical stream of molten metal[6]. Various components of the atomizer and their final assembly is shown in Fig. 3.4. The inlet for the atomizing gas is provided in the upper portion of the atomizer which also contains a common hollow space (Fig. 3.4(a)). To this upper portion of the atomizer a removable type disk containing six symmetric holes (Fig. 3.4(c)) is connected. In between the

upper block and the disk a pressure ring (Fig. 3.4(b)) is placed. The common hollow space and the pressure ring helps in maintaining uniformity of pressure in each jet. This design was, however, found unsatisfactory as it was observed that after about 10 - 12 seconds after starting the atomization process the molten metal stream passage was completely clogged. This was attributed to the fact that the highly pressurized air jets caused a lot of splashing of molten metal. Due to this splashing some of the atomized particles moved upwards and caught the cold surface of the atomizer and got solidified on the metal passage opening. One of the ways of avoiding the clogging was to increase the distance between the impingement point and the atomizer surface. This could be achieved either by increasing the diameter of the atomizer, that is, increasing the distance between the opposite jets, or by decreasing the angle of the jets with the vertical axis, i.e. with the metal stream. Both the means could be equally effective but because of the simplicity and to be able to use the previous set-up only the latter was chosen. The jet angles could be easily decreased just by changing the angle of the tapered hole in the atomizer disc. Three similar atomizer discs with 1/10" diameter jets and 15^{o}, 25^{o}, and 35^{o} jet angles with the vertical axis, respectively, were fabricated. These now provided a means to study the effect of atomizing angle also on the atomization process.

3.1.3.3 Nozzle-atomizer assembly: The final nozzle - atomizer assembly is schematically shown in Fig. 3.2. Stainless steel nozzle of desired opening diameter was placed on one of the steps of the two step hole at the bottom of the graphite crucible. It could then be connected to the atomizer through a stainless steel tube which rested on the second step, below the nozzle, in the crucible, and whose outer surface near the bottom portion was threaded.

3.1.4 Stopper Rod

An 8 mm diameter, 400 mm length stainless steel rod having a 'V' shaped bottom, which could be seated in the 'V' shaped cavity of nozzle served as a stopper rod (Fig. 3.2). When it seated in the cavity, it provided a water tight leak proof contact, and when lifted allowed the molten metal to pass through the nozzle.

3.1.5 Water Tank

An aluminium tank, filled with water was kept 3 to 4 feet below the furnace to quench and collect the atomized particles.

3.2 EXPERIMENTAL PROCEDURE

3.2.1 Preparation of Charge

The charge consisted of small granules of the metal to be atomized and the rejected coarse fractions of previous trials. The charge material was properly cleaned to exclude metal oxides and ceramic particles and then dried to remove moisture.

3.2.2 Procedure

To start the experiments first of all the set-up was assembled. After properly cleaning the nozzle with the sand paper it was placed along with the stainless steel tube in the graphite crucible which acted as a container. The alignment of nozzle was checked with water. The 'V' shaped bottom of the stopper rod was tightly fitted in the 'V' shaped cavity of the nozzle, and tested with water for any possible leakage. This assembly was then introduced in the furnace after the inside of the furnace was properly cleaned and the bottom of the furnace was levelled horizontally with a spirit level. The atomizer was then connected to the nozzle through the steel tube. The atomizer was connected to a compressor or a gas cylinder through rubber tubings. The tank which was placed below the furnace assembly to collect and quench the metal droplets was filled with water. Already prepared charge was introduced into the

crucible and the top of the furnace was covered with asbestos sheets. A chromel-alumel thermocouple was introduced into the furnace from the top and kept at a fixed position outside the graphite crucible. This thermocouple, which was connected to the temperature controller, was calibrated against another chromel-alumel thermocouple which could be introduced into the furnace from the top whenever desired and kept inside the graphite crucible. The calibrated thermocouple could measure the temperature of the molten metal within $\pm$ 5 ^{o}C accuracy. As the second thermocouple caused some inconvenience during the experimentation, it was not used in most of the actual runs, and the temperature of the molten metal was measured with the help of the calibrated thermocouple only. However, the calibration of the former thermocouple was checked from time to time. After properly positioning the thermocouple the furnace was slowly heated up. When the desired temperature was reached and maintained for about half an hour, the stopper rod was lifted up and the air compressor's valve was opened to supply compressed air at about 70 psi. The molten metal which came out of the nozzle was atomized by air jets and the fine croplets were quenched and collected in the water tank at the bottom of the atomization unit. After the run was over the compressor was switched off and the powder was removed from the tank and after drying it was subjected to sieve analysis.

The sieve analysis was carried out using a standard set of BSS sieves. The weights of initial sample and powder retained on individual sieves after the sieving were carefully determined.

In all, about 40 experiments were performed with an objective to study the effect of variation in nozzle diameter, atomizing angle, temperature, and the type of material on the atomization behaviour, viz. average size and size distribution of the particles. These experiments can be broadly divided into three main categories depending on the material being automized.

In the first category about sixteen experiments were performed using tin as the metal to be atomized at three different temperatures, namely, 285 °C, 315 °C, and 375 °C. At 285 °C three experiments using three different nozzles (0.1295 cm, 0.183 cm, and 0.236 cm) were performed using 25° atomizing angle. At 315 °C nine experiments were performed using the three nozzles and three atomizing angles, namely, 15°, 25°, and 35°. At the same temperature one more experiment was performed using a nozzle of 0.236 cm diameter and atomizer with 45° angle. This particular atomizer was not used in any of the subsequent experiments because of the clogging of the atomizer, which has already been discussed above. At 375 °C three experiments using nozzles of three different diameters and 25° atomizer were performed.

In the second category of experiments, in which lead was the metal to be atomized, all nine experiments were performed at 375 °C only using all three nozzles and the three atomizers (15°, 25°, and 35°).

A few experiments were also performed using lead-tin eutectic alloy. In this set of experiments which constituted the third category of experiments the alloy was atomized at four different temperatures, namely, 285 °C, 315 °C, 345 °C, and 375 °C using all the three nozzles and 25° atomizer.

The results of these experiments are presented and discussed in the following chapter.

CHAPTER 4

RESULTS AND DISCUSSION

4.1 RESULTS

Total number of experiments that have been performed in this study can be classified into three categories. In the first category of experiments, using tin as the metal to be atomized, the effect of nozzle diameter, metal temperature, and atomizing angle on average particle size and size distribution has been studied. In the second category lead has been employed as the metal to be atomized and the effect of nozzle diameter and the atomizing angle investigated. A binary lead-tin eutectic alloy constituted the material in the third category of experiments. In this category, the experiments have been performed to study the effect of nozzle diameter and material temperature. Metal powder obtained after atomization was sieved using a standard set of BSS sieves after properly drying the powder. The powder retained on each sieve was then weighed. Table 4.1 gives the opening sizes of the various sieves, and the average sizes of the two consecutive sieves used for sieving purpose.

The experimental data has been compiled in the form of weight of powder retained on each of the sieves used for sieving in grammes which then converted into

TABLE 4.1

Opening Sizes and Average Sizes of BSS Sieves Used

Sieve No.	Opening size in mm	Average size in mm	X_i	Log X_i
+ 72	- /0.211	0.254	0.211	-
- 72 + 100	0.211/0.151	0.181	0.151	-0.8210
-100 + 150	0.151/0.104	0.128	0.104	-0.9830
-150 + 200	0.104/0.075	0.090	0.075	-1.1249
-200 + 300	0.075/0.053	0.064	0.053	-1.2757
-300	0.053/ -	0.035	-	-

X_i is the opening size of the sieve on which material is retained.

weight percentage retained and cumulative weight percentage retained. The data for the various experiments performed during this investigation is presented in tabular form in Tables 4.2 to 4.14. Tables 4.2 to 4.7 are the compilation of the data for tin atomized under different operating conditions, Tables 4.8 to 4.10 are the compilation of similar data for lead, where as for lead-tin eutectic alloy the data is tabulated in Tables 4.11 to 4.14.

The effect of three nozzle diameters, namely, 0.236 cm, 0.183 cm, and 0.1295 cm on the atomization of molten tin at 285 ^{o}C using an atomizer in which each of the six air jets forms an angle of 25^{o} with the vertical metal stream (atomizing angle) is presented in Table 4.2.

Tables 4.3, 4.4, and 4.5 present the effect of three nozzle diameters (as mentioned above) on atomization of tin at 315 ^{o}C using an atomizing angle of 15^{o}, 25^{o}, and 35^{o}, respectively.

As it has already been pointed out in last chapter, an atomizer in which the air jets formed an angle of 45^{o} with the metal stream resulted in clogging of the atomizer after around 8 to 10 seconds. Therefore, only one experiment was performed using this atomizer, the data for which is presented in Table 4.6.

The data for atomization of tin at 375 ^{o}C using an atomizing angle of 25^{o} for the three different nozzles

TABLE 4.2

Experimental Data for Atomization of Tin at 285°C Using Atomizer of 15° Angle For Three Different Nozzles.

Material: Tin Temperature: 285 °C Atomizing angle 25°

Sieve No	Nozzle dia. = 0.236 cm			Nozzle dia = 0.183 cm			Nozzle dia = 0.1295 cm		
	Weight retained in gms	Weight % retained	Cumulative weight % retained	Weight retained in gms	Weight % retained	Cumulative weight % retained	Weight retained in gms	Weight % retained	Cumulative weight % retained
+ 72	43.526	33.29	33.29	36.949	32.64	32.64	30.043	31.01	31.01
- 72 + 100	50.021	38.26	71.55	42.003	37.10	69.74	36.203	37.37	68.38
-100 + 150	19.123	14.63	86.18	17.724	15.66	85.40	15.922	16.44	84.82
-150 + 200	9.042	6.92	93.10	8.043	7.10	92.50	7.023	7.25	92.07
-200 + 300	6.432	4.92	98.02	6.105	5.39	97.89	5.534	5.71	97.78
-300	2.603	1.99	100.00	2.392	2.11	100.00	2.147	2.22	100.00

TABLE 4.3

Experimental Data for Atomization of Tin at 315 °C Using Atomizer of 15° Angle For Three Different Nozzles.

Material: Tin Temperature: 315 °C Atonizing angle: 15°

Sieve No.	Nozzle dia = 0.236 cm			Nozzle dia = 0.183 cm			Nozzle dia = 0.1295 cm		
	Weight retained in gms	Weight % retained	Cumulative weight % retained	Weight retained in gms	Weight % retained	Cumulative weight % retained	Weight retained in gms	Weight % retained	Cumulati weight % retained
+ 72	21.353	40.42	40.42	19.819	35.68	35.68	6.177	38.51	38.51
-72 + 100	22.142	41.92	82.34	22.170	39.91	75.59	6.474	40.37	78.88
-100 + 150	6.284	11.90	94.24	7.908	14.24	89.83	1.990	12.41	91.29
-150 +200	1.490	2.82	97.06	2.525	4.55	94.38	0.725	4.52	95.81
-200 +300	1.178	2.21	99.27	2.391	4.30	98.68	0.436	2.72	98.53
-300	0.387	0.73	100.00	0.735	1.32	100.00	0.236	1.47	100.00

TABLE 4.4

Experimental Data for Atomization of Tin at 315 °C Using Atomizer of 25° Angle for Three Different Nozzles

Material : Tin Temperature: 315°C Atomizing angle: 25°

Seive No	Nozzle dia. = 0.236 cm			Nozzle dia = 0.183 cm			Nozzle dia = 0.1295 cm		
	Weight retained in gms	Weight % retained	Cumulative weight % retained	Weight retained in gms	Weight % retained	Cumulative weight % retained	Weight retained in gms	Weight % retained	Cumulat weight retaine
+ 72	41.434	28.24	28.24	36.289	27.99	27.99	25.974	23.86	23.86
- 72 + 100	57.420	39.13	67.37	50.324	38.81	66.80	43.822	40.26	64.12
-100 + 150	24.673	16.81	84.18	22.203	17.12	83.92	19.636	18.04	82.16
-150 + 200	12.031	8.19	92.37	10.688	8.24	92.16	9.848	9.05	91.21
-200 + 300	8.432	5.75	98.12	7.306	5.63	97.79	7.250	6.66	97.87
-300	2.758	1.88	100.00	2.852	2.20	100.00	2.310	2.12	100.00

TABLE 4.5

Experimental Data for Atomization of Tin at 315 °C Using Atomizer of 35° Angle for Three Different Nozzles

Material : Tin Temperature: 315 °C Atomizing angle: 35°

Sieve No.	Nozzle dia. = 0.236 cm			Nozzle dia. = 0.183 cm			Nozzle dia = 0.1295 cm		
	Weight retained in gms.	Weight % retained	Cumulative weight % retained	Weight retained in gms.	Weight % retained	Cumulative weight % retained	Weight retained in gms	Weight % retained	Cumulati weight % retaine
+ 72	61.808	28.02	28.02	53.991	19.30	19.30	12.946	9.71	9.71
- 72 + 100	83.625	37.91	65.93	100.104	35.78	55.08	28.000	21.01	30.72
-100 + 150	37.725	17.10	83.03	54.185	19.37	74.45	25.965	19.48	50.20
-150 + 200	20.314	9.21	92.24	35.243	12.60	87.05	24.370	18.28	68.48
-200 + 300	12.608	5.72	97.96	23.228	8.30	95.35	22.401	16.81	85.29
-300	4.492	2.02	100.00	13.017	4.65	100.00	19.609	14.71	100.00

TABLE 4.6

Experimental Data for Atomization of Tin at 315 °C Using Atomizer of 45° Angle For a Nozzle of 0.236 cm Diameter.

Material : Tin

Temperature : 315 °C

Atomizing angle: 45°

Sieve No.	Nozzle dia. = 0.236 cm		
	Weight retained in gms	Weight % retained	Cumulative weight % retained
+ 72	27.127	18.77	18.77
- 72 + 100	29.007	20.08	38.85
-100 + 150	27.195	18.81	57.66
-150 + 200	11.166	7.57	65.23
-200 + 300	33.820	23.36	88.59
-300	16.337	11.41	100.00

Experimental Data for Atomization of Tin At 375 °C Using Atomizer of 25° Angle for Three Different Nozzles.

Material : Tin Temperature : 375 °C Atomizing angle: 25°

Sieve No.	Nozzle dia. = 0.236 cm			Nozzle dia. = 0.183 cm			Nozzle dia. = 0.1295 cm		
	Weight retained in gms	Weight % retained	Cumulative weight % retained	Weight retained in gms	Weight % retained	Cumulative weight % retained	Weight retained in gms	Weight % retained	Cumulat weight retaine
+ 72	39.174	26.28	26.28	36.062	26.39	26.39	19.820	23.74	23.74
- 72 + 100	57.779	38.77	65.05	51.622	37.78	64.17	31.213	37.39	61.13
-100 + 150	26.120	17.53	82.58	24.115	17.67	81.82	15.978	19.14	80.27
-150 + 200	14.370	9.64	92.22	12.285	8.99	90.81	7.189	8.61	88.88
-200 + 300	6.615	4.44	96.66	8.530	6.28	97.09	6.058	7.26	96.14
-300	4.986	3.35	100.00	3.967	2.90	100.00	3.217	3.85	100.00

TABLE 4.8

Experimental Data for Atomization of Lead at 375 °C Using Atomizer of 15° Angle for Three Different Nozzles.

Material: Lead Temperature: 375 °C Atomizing angle: 15°

Sieve No.	Nozzle dia. = 0.236 cm			Nozzle dia. = 0.183 cm			Nozzle dia. = 0.1295 cm		
	Weight retained in gms	Weight % retained	Cumulative weight % retained	Weight retained in gms	Weight % retained	Cumulative weight % retained	Weight retained in gms	Weight % retained	Cumulativ weight% retained
+ 72	46.697	41.32	41.32	35.194	36.16	36.16	16.836	37.98	37.98
- 72 + 100	44.955	39.78	81.10	40.057	41.15	77.31	19.400	43.76	81.74
-100 + 150	12.285	10.87	91.97	6.378	6.55	83.86	1.763	3.98	85.72
-150 + 200	2.920	2.58	94.55	9.720	9.99	93.85	2.906	6.56	92.28
-200 + 300	5.460	4.83	99.38	4.973	5.11	98.96	3.107	7.01	99.29
-300	0.704	0.62	100.00	1.013	1.04	100.00	0.318	0.72	100.00

TABLE 4.9

Experimental Data for Atomization of Lead at 375 °C Using Atomizer of 25° Angle for Three Different Nozzles.

Material: Lead Temperature: 375 °C Atomizing angle: 25°

Sieve No.	Nozzle dia. = 0.236 cm			Nozzle dia. = 0.183 cm			Nozzle dia. = 0.1295 cm		
	Weight retained in gms.	Weight % retained	Cumulative weight % retained	Weight retained in gms.	Weight % retained	Cumulative Weight % retained	Weight retained in gms.	Weight % retained	Cumulative weight % retained
+ 72	125.610	29.37	29.37	65.792	28.39	28.39	50.860	27.28	27.28
- 72 + 100	163.993	38.44	67.71	89.402	38.58	66.97	74.511	39.96	67.24
-100 + 150	29.086	6.80	74.51	8.122	3.51	70.48	8.467	1.86	69.10
-150 + 200	60.324	14.10	88.61	33.361	14.40	84.88	21.842	11.71	80.81
-200 + 300	38.942	9.11	97.72	26.076	11.25	96.13	31.846	16.81	97.62
-300	9.743	2.28	100.00	8.960	3.87	100.00	4.444	2.38	100.00

TABLE 4.10

Experimental Data for Atomization of Lead at 375 °C Using Atomizer of 35° Angle for Three Different Nozzles.

Material: Lead Temperature: 375 °C Atomizing Angle: 35°

Sieve No.	Nozzle dia. = 0.236 cm			Nozzle dia. = 0.183 cm			Nozzle dia. = 0.1295 cm		
	Weight retained in gms	Weight % retained	Cumulative weight % retained	Weight retained in gms	Weight % retained	Cumulative weight % retained	Weight retained in gms	Weight % retained	Cumulative weight % retained
+ 72	102.206	27.05	27.05	84.393	18.55	18.55	13.734	7.51	7.51
- 72 + 100	140.341	37.14	64.19	160.724	35.33	53.88	33.390	18.27	25.78
-100 + 150	75.107	19.88	84.07	92.174	20.26	74.14	40.942	22.40	48.18
-150 + 200	18.932	5.01	89.08	38.491	8.46	82.60	33.471	18.31	66.49
-200 + 300	34.243	9.06	98.14	60.258	13.25	95.85	36.004	19.70	86.19
-300	6.998	1.85	100.00	18.842	4.14	100.00	25.253	13.82	100.00

TABLE 4.11

Experimental Data for Atomization of Lead-Tin Alloy at 285 °; Using Atomizer of 25° Angle for Three Different Nozzles.

Material: Tin-Lead eutectic alloy Temperature: 285 °C Atomizing angle: 25°

Sieve No	Nozzle dia. = 0.236 cm			Nozzle dia. = 0.183 cm			Nozzle dia. = 0.1295 cm		
	Weight retained in gms	Weight % retained	Cumulative weight % retained	Weight retained in gms	Weight % retained	Cumulative weight % retained	Weight retained in gms	Weight % retained	Cumulative weight % retained
+ 72	68.953	32.47	32.47	49.043	26.51	26.51	30.016	26.78	26.78
- 72 + 100	80.207	37.77	70.24	67.543	36.51	63.02	42.620	38.03	64.81
-100 + 150	32.323	15.22	85.46	34.139	18.45	81.47	15.213	13.57	78.38
-150 + 200	16.704	7.87	93.33	20.996	11.35	92.82	11.550	10.31	88.69
-200 + 300	10.120	4.77	98.10	10.344	5.59	98.41	8.006	7.14	95.83
-300	4.053	1.91	100.00	2.937	1.59	100.00	4.671	4.17	100.00

TABLE 4.12

Experimental Data for Atomization of Lead-Tin Alloy at 315 °C Using Atomizer of 25° Angle for Three Different Nozzles.

Material: Tin -Lead eutectic alloy Temperature: 315 °C Atomizing angle: 25°

Sieve No.	Nozzle dia. = 0.236 cm			Nozzle dia. = 0.183 cm			Nozzle dia. = 0.1295 cm		
	Weight retained in gms	Weight % retained	Cumulative weight % retained	Weight retained in gms	Weight % retained	Cumulative weight % retained	Weight retained in gms.	Weight % retained	Cumulative weight % retained
+ 72	90.978	27.39	27.39	70.705	24.44	24.44	34.884	23.34	23.34
- 72 + 100	123.516	37.18	64.57	106.020	36.65	61.09	54.521	36.48	59.82
-100 + 150	57.481	17.30	81.87	54.624	18.88	79.97	28.356	18.97	78.79
-150 + 200	32.348	9.74	91.61	30.442	10.52	90.49	16.958	11.35	90.14
-200 + 300	17.005	5.12	96.73	18.527	6.41	96.90	9.332	6.24	96.38
-300	10.890	3.28	100.00	8.938	3.09	100.00	5.416	3.62	100.00

TABLE 4.13

Experimental Data for Atomization of Lead-Tin Alloy at 345 °C Using Atomizer of 25° Angle for Three Different Nozzles.

Material: Tin-Lead eutectic alloy Temperature: 345 °C Atomizing angle: 25°

Sieve No	Nozzle dia. = 0.236 cm			Nozzle dia. = 0.183 cm			Nozzle dia. = 0.1295 cm		
	Weight retained in gms.	Weight % retained	Cumulative weight % retained	Weight retained in gms.	Weight % retained	Cumulative weight % retained	Weight retained in gms.	Weight % retained	Cumulative weight % retained
+ 72	66.504	25.17	25.17	58.927	26.97	26.97	32.183	21.32	21.32
- 72 + 100	102.990	38.98	64.15	86.942	39.79	66.76	54.600	36.17	57.49
-100 + 150	38.207	14.46	78.61	21.911	12.78	79.54	24.818	16.44	73.93
-150 + 200	28.749	10.88	89.49	20.741	9.49	89.03	20.201	13.38	87.31
-200 + 300	21.217	8.03	97.52	14.266	6.53	95.56	15.262	10.11	97.42
-300	6.569	2.49	100.00	9.690	4.44	100.00	3.872	2.57	100.00

TABLE 4.14

Experimental Data for Atomization of Lead-Tin Alloy at 375 °C Using Atomizer of 25° Angle for Three Different Nozzles.

Material: Tin-Lead eutectic alloy Temperature: 375 °C Atomizing angle: 25°

Sieve No	Nozzle dia. = 0.236 cm			Nozzle dia. = 0.183 cm			Nozzle dia. = 0.1295 cm		
	Weight retained in gms.	Weight % retained	Cumulative weight % retained	Weight retained in gms.	Weight % retained	Cumulative weight % retained	Weight retained in gms.	Weight % retained	Cumulative weight % retained
+ 72	74.269	21.77	21.77	55.157	19.86	19.86	41.195	20.46	20.46
-72 + 100	130.726	38.31	60.08	101.183	36.44	56.30	73.653	36.58	57.04
-100 + 150	58.919	17.27	77.35	55.687	20.05	76.35	39.520	19.63	76.67
-150 + 200	39.739	11.65	89.00	33.745	12.15	88.56	24.011	11.92	88.59
-200 + 300	26.298	7.71	96.70	20.585	7.41	95.91	13.703	6.82	95.40
-300	11.273	3.30	100.00	11.317	4.08	100.00	9.282	4.61	100.00

is compiled in Table 4.7.

Tables 4.8 to 4.10 present the data for atomization of lead at 375 °C for the three nozzles using atomizers of three different atomizing angles, namely, 15°, 25°, and 35°, respectively.

Table 4.11 is the compilation of data for atomization of lead-tin eutectic alloy at 285 °C for the three nozzle diameters using an atomizing angle of 25°. Tables 4.12, 4.13, and 4.14 present similar data at three different temperatures, viz., 315 °C, 345 °C, and 375 °C, respectively.

4.2 DISCUSSION

4.2.1 Powder Size Distribution

To describe the size distribution for a system like this in which the number of particles are extremely large, the most practical approach is the weight basis. The very first look at the weighed sieve fractions clearly revealed that the size distribution was invariably assymmetrical in nature.

A number of distributions were tried to fit the data and was found that the log-normal distribution fitted with the data best. The cumulative weights retained when plotted on log-probability paper resulted in

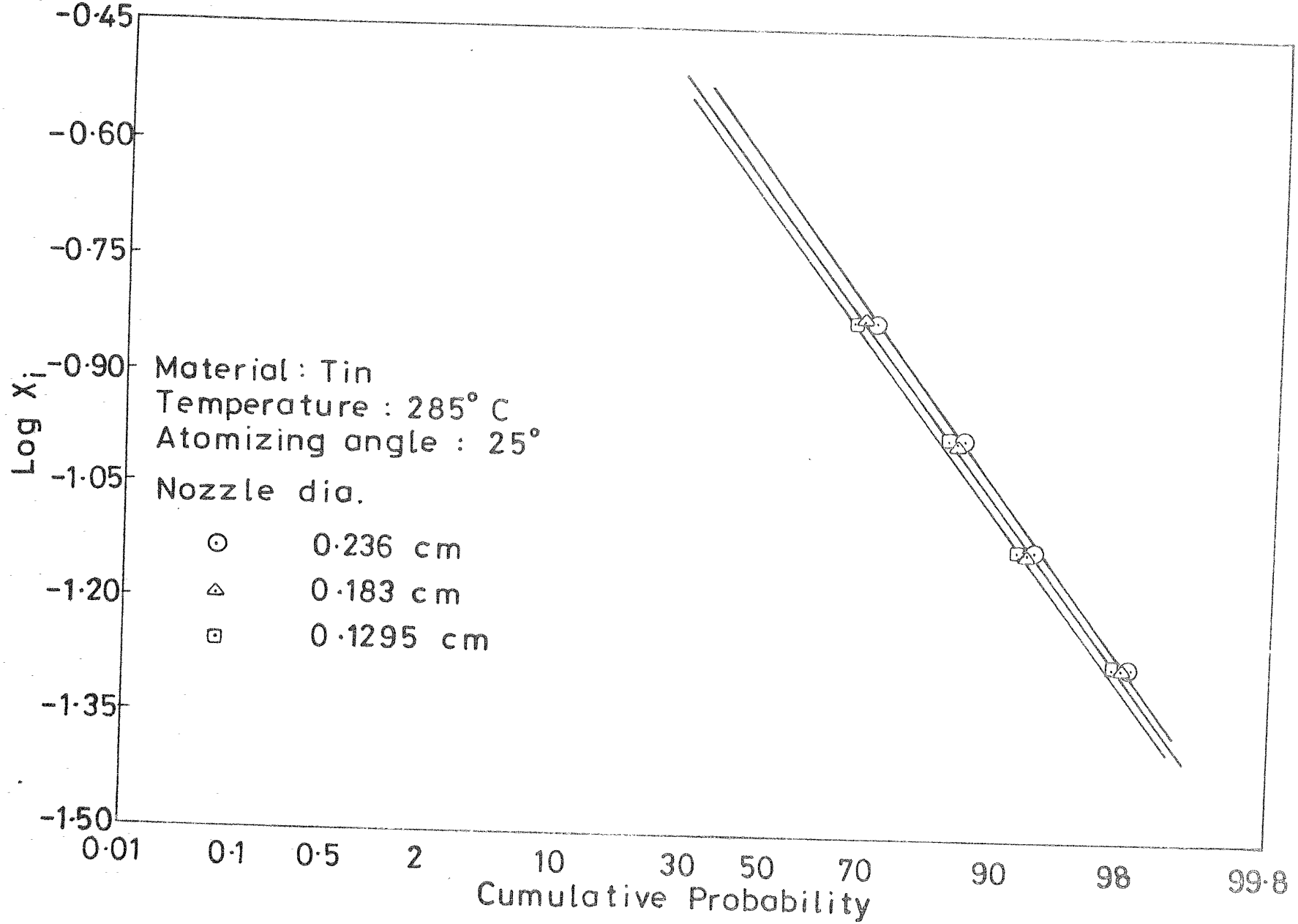

Fig. 4·1 Effect of nozzle diameter on size distributio

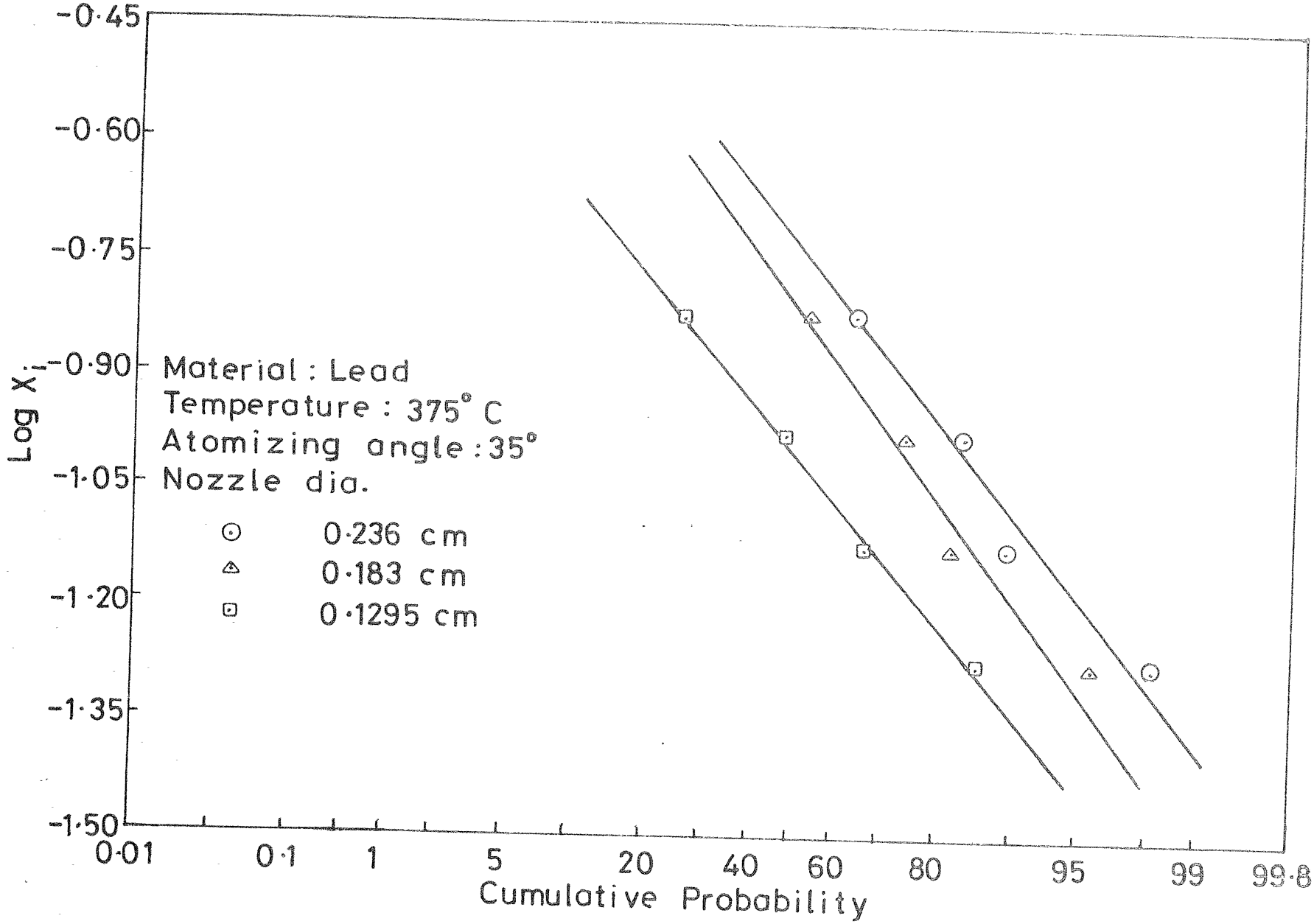

Fig. 4·2 Effect of nozzle diameter on size distribution

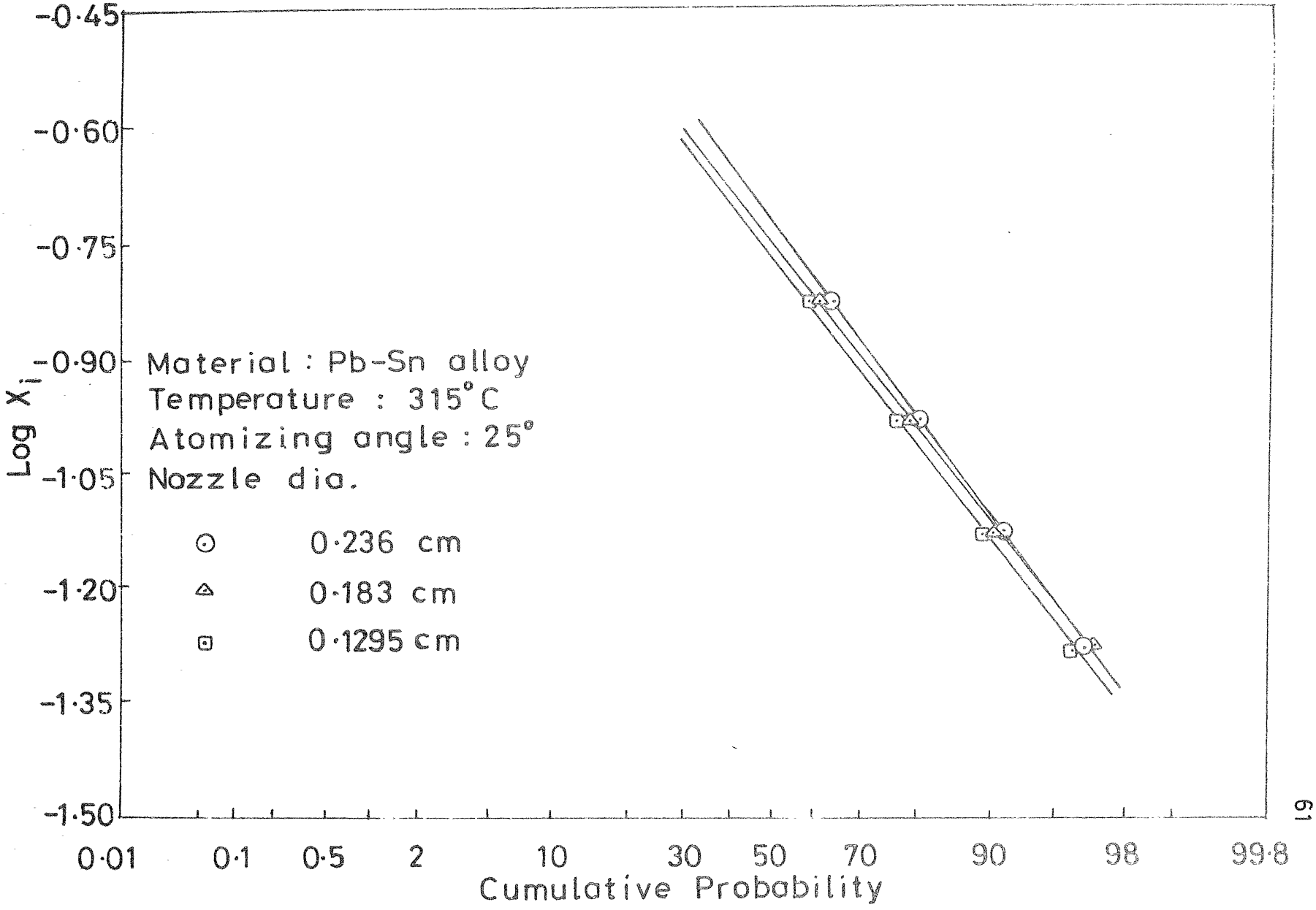

Fig. 4·3 Effect of nozzle diameter on size distribution

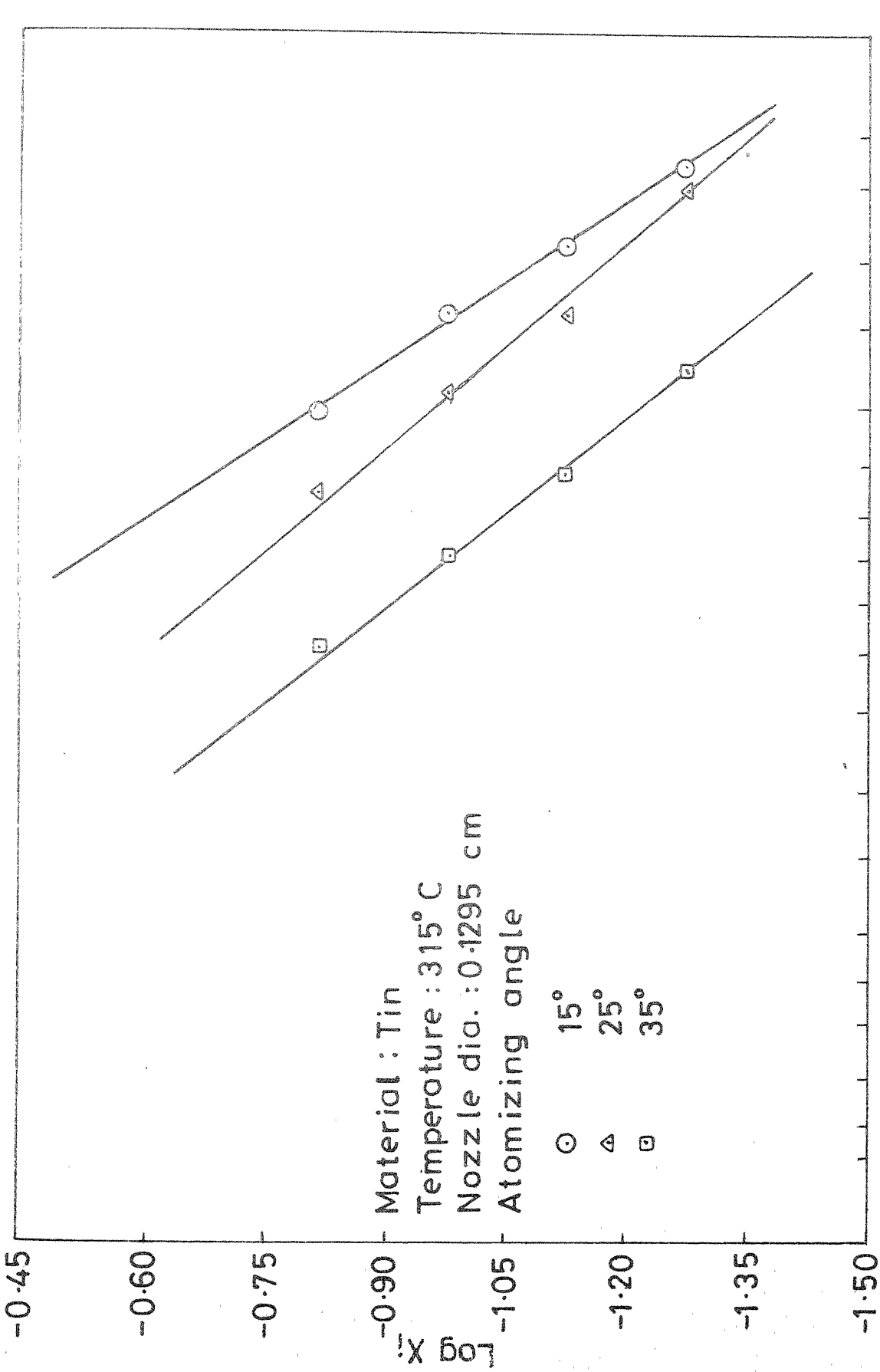

Fig.4.4 Effect of atomizing angle on size distribution

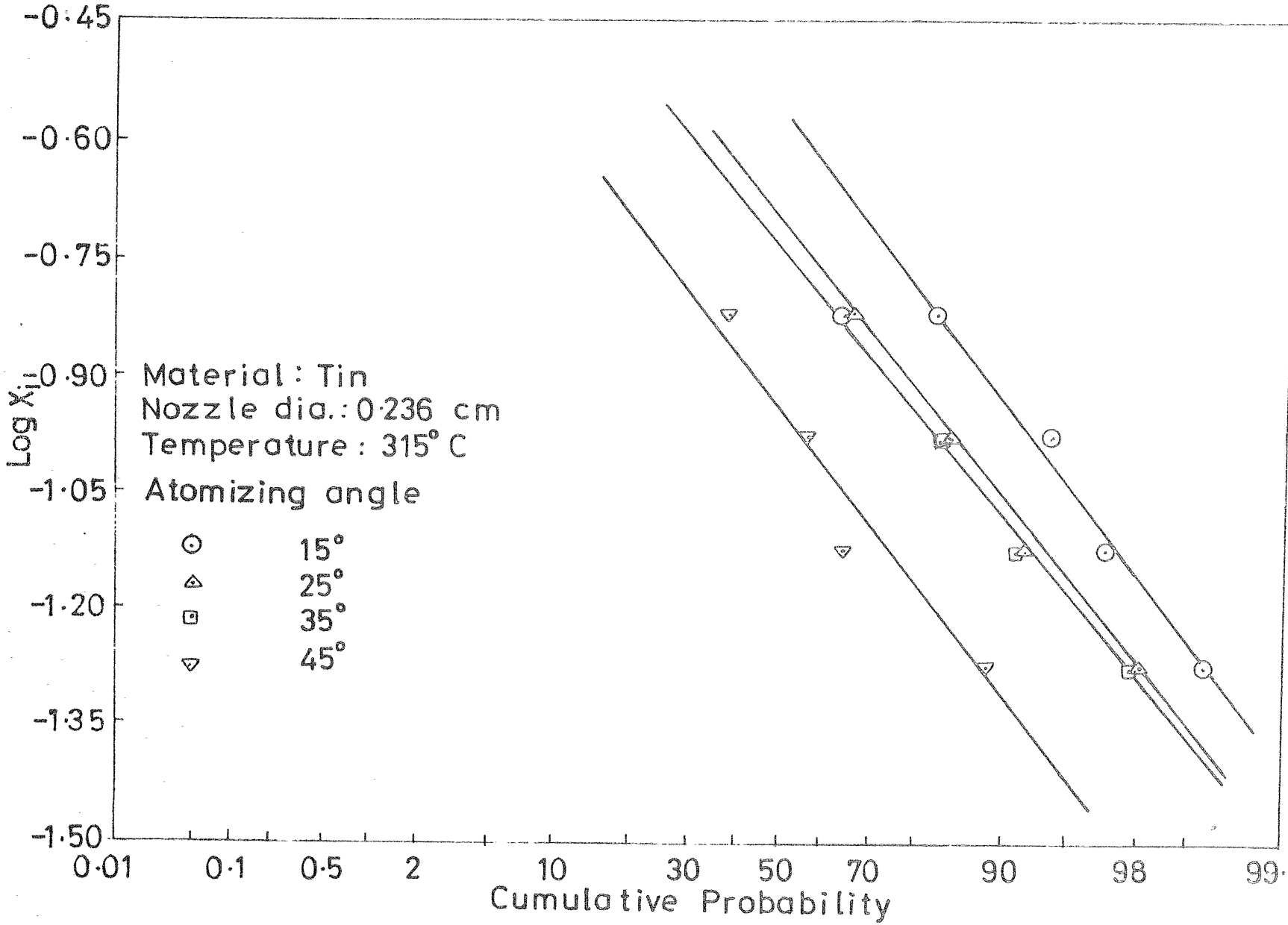

Fig. 4·5 Effect of atomizing angle on size distribution

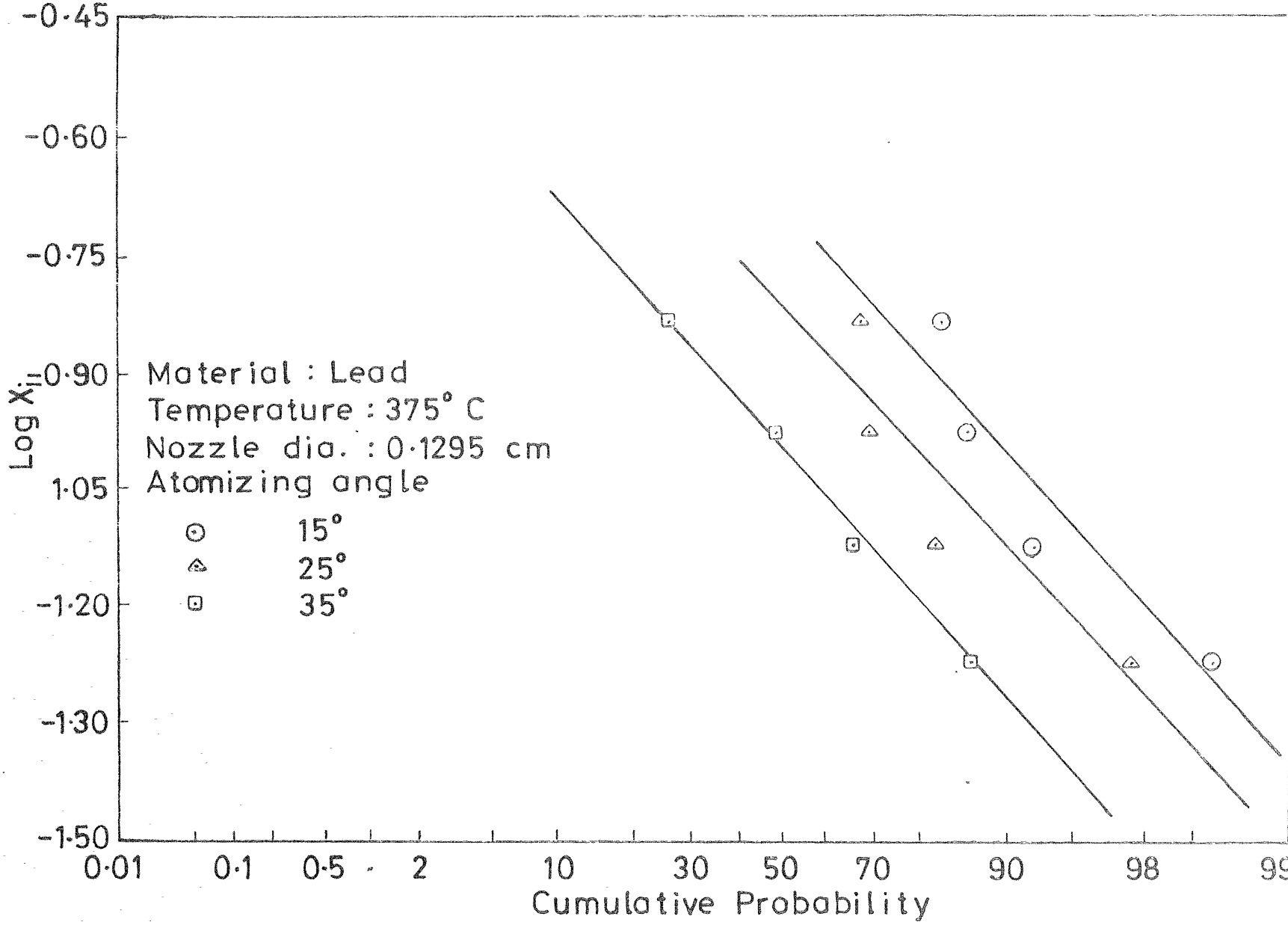

Fig. 4·6 Effect of atomizing angle on size distribution

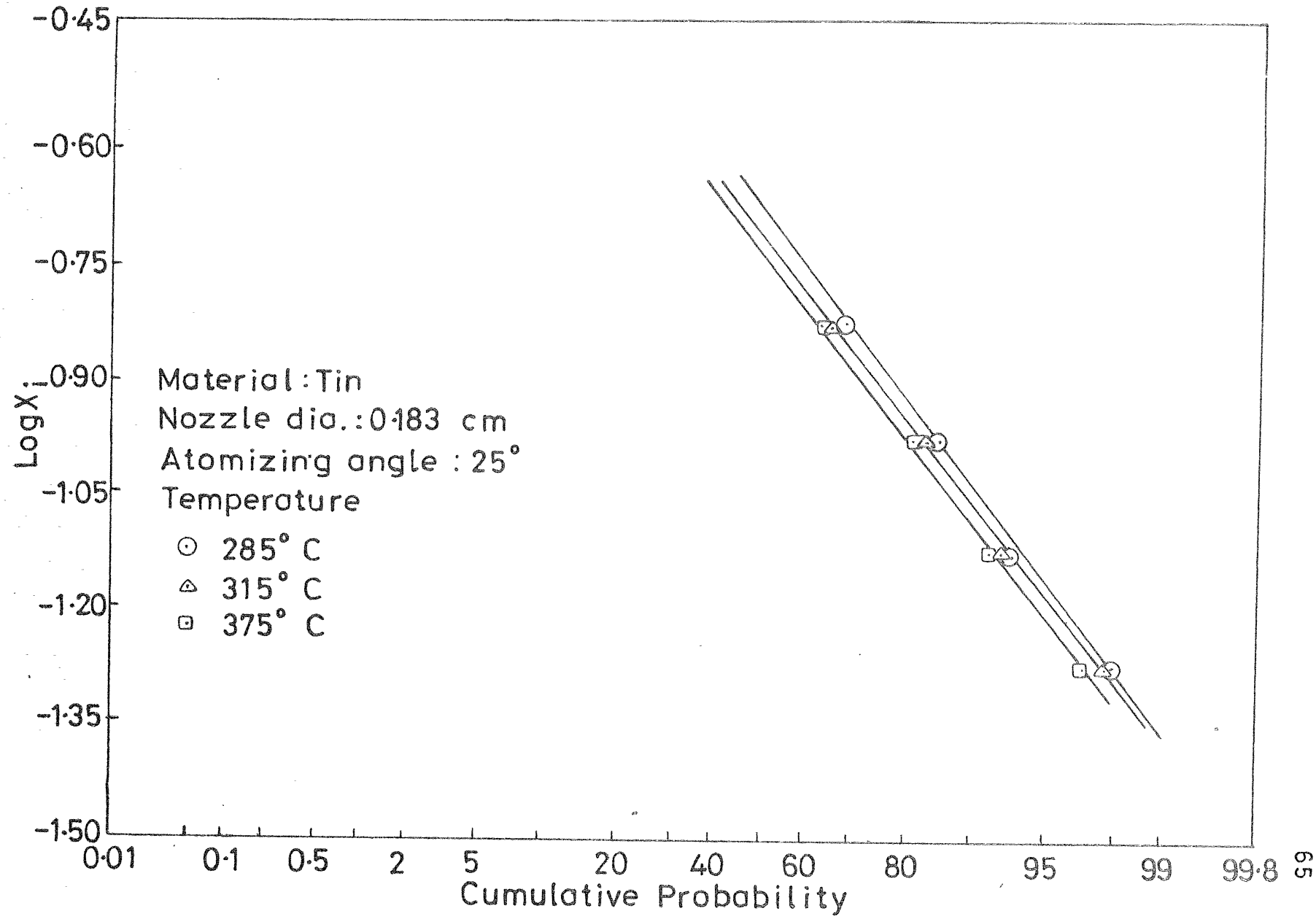

Fig. 4·7 Effect of temperature on size distribution

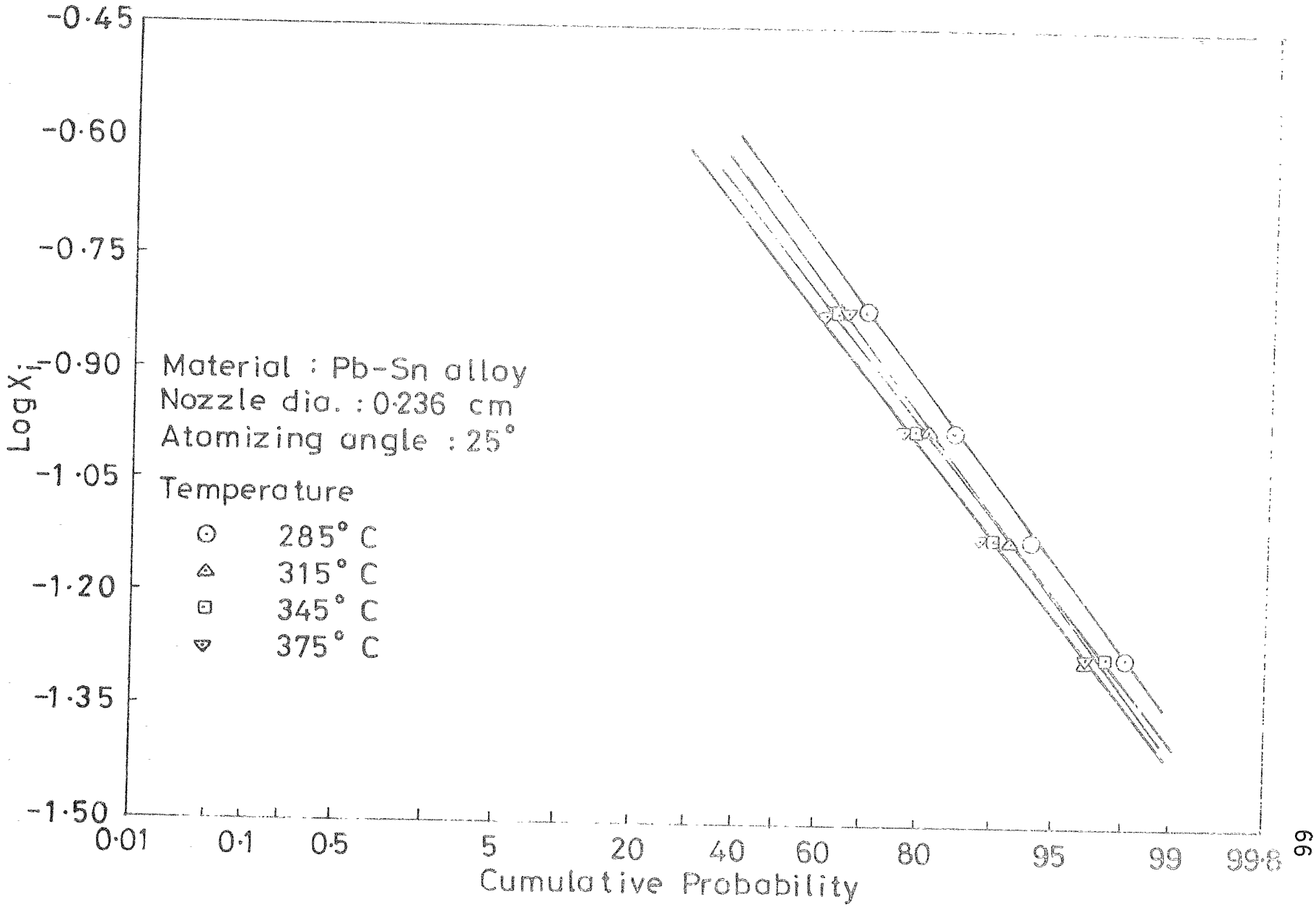

Fig. 4·8 Effect of temperature on size distribution

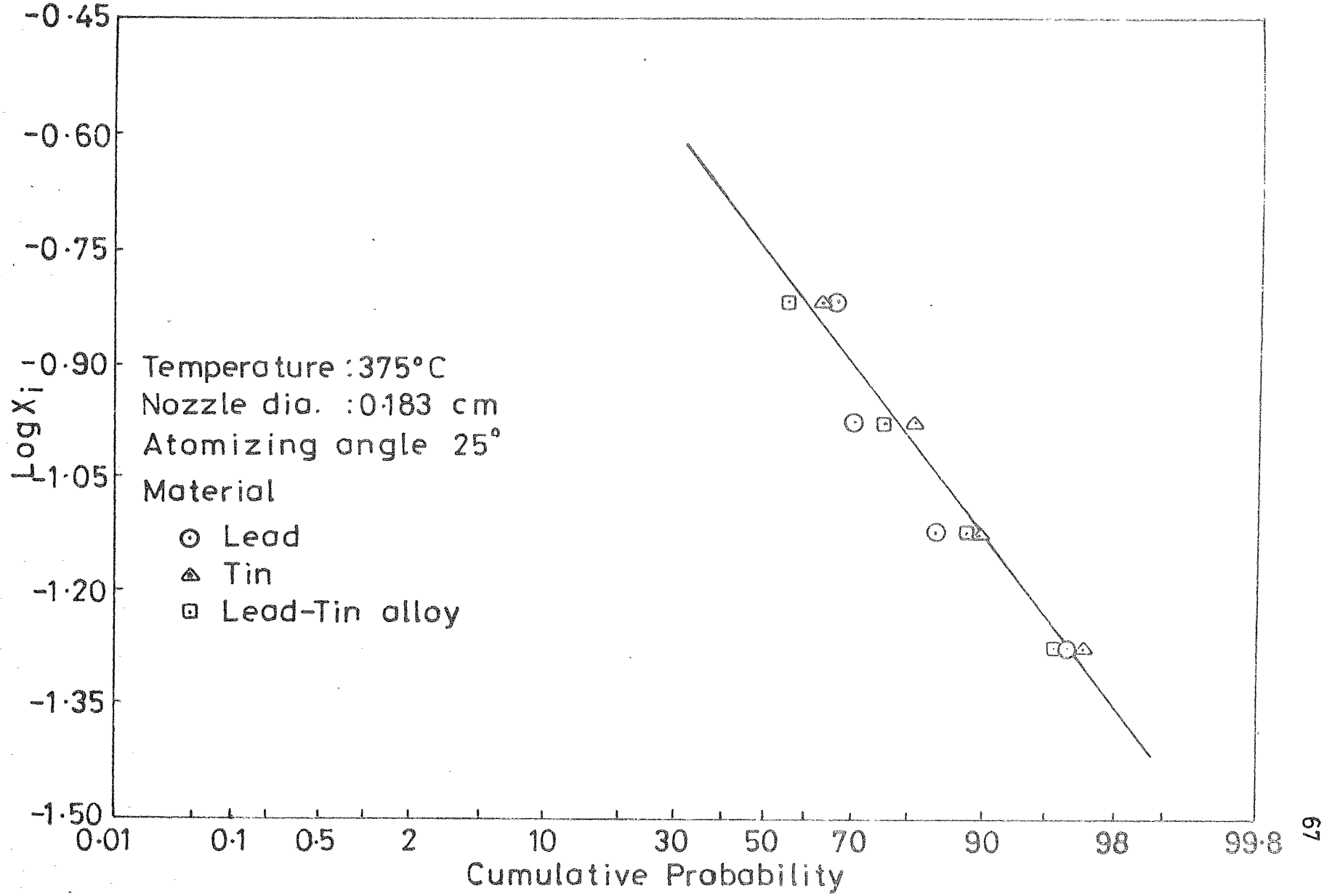

Fig. 4·9 Effect of material on size distribution

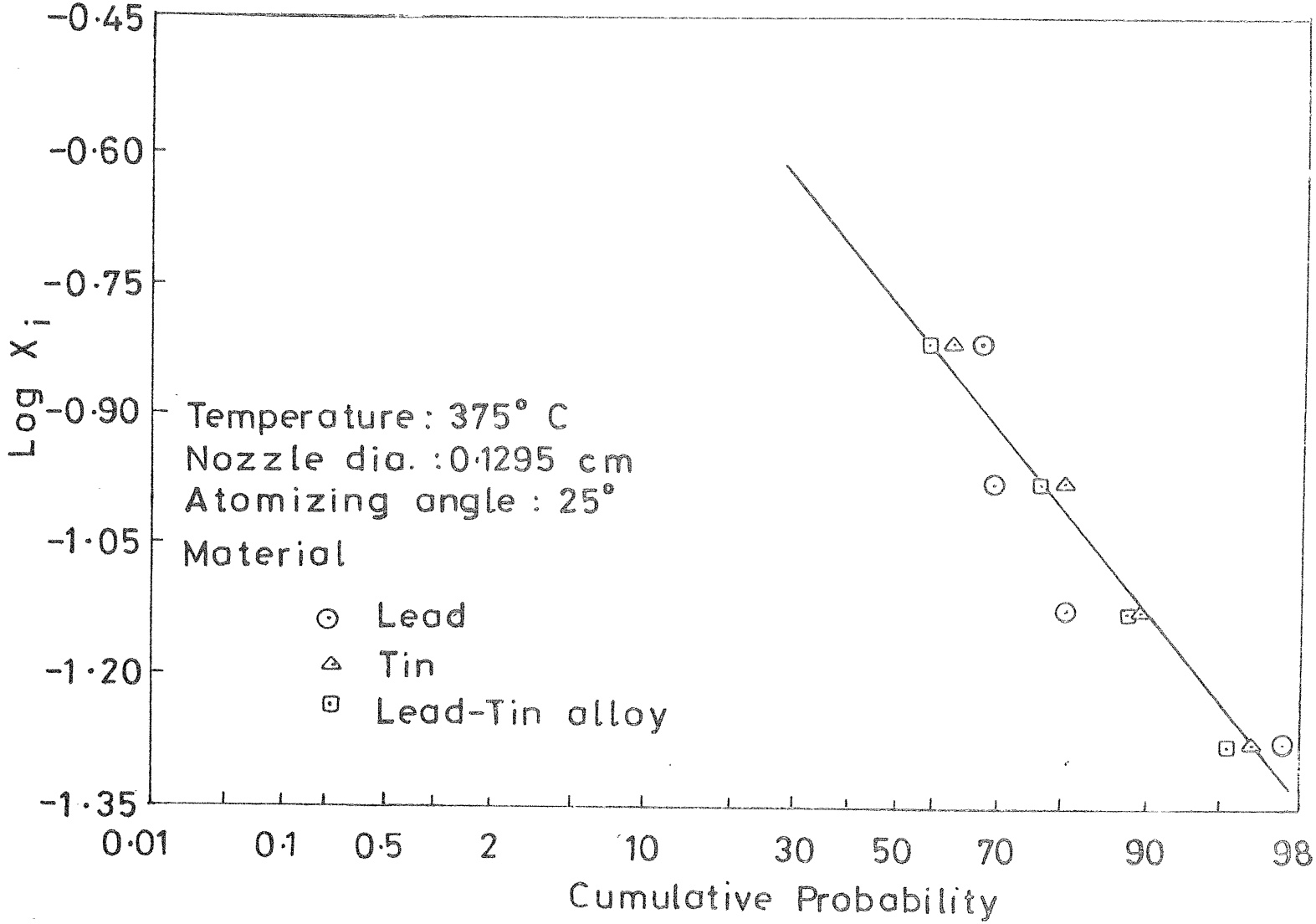

Fig. 4·10 Effect of material on size distribution

consecutive sieves, the average size of these sieves being $\bar{X}_i$.

In the cumulative plots in Figures 4.1 to 4.10 data points for sieve number below 72 and above 300 have not been included for the following reasons. It was observed that during atomization process some powder was formed due to processes other than atomization, viz., dripping of metal etc. Also, it was observed that the air compressor that was used in the set-up could give an air blow at a reasonably constant pressure only for about 20 seconds after which the pressure rapidly went down. In the present investigation only that powder that was produced at a constant pressure is considered. It was observed that the major portion of the powder produced after 20 seconds was coarser than the opening size of the sieve number 52. It was therefore assumed that the powder that was coarser than the sieve 52 was due to processes other than atomization of molten stream at a desired constant pressure. It was further assumed that the weight of the coarser particles which were formed due to actual atomization but not included in the data would be compensated by the weight of the finer particles produced due to other processes but was not included in the data. To include the first and the last data points in the calculation of mean size the average size for - 300 particles has been taken as

0.035 mm and that for + 72 is 0.254 mm. The mean sizes thus evaluated are tabulated in Table 4.15. The mean size values thus evaluated compare well with the graphical values in most of the cases.

4.2.3 Application of Previous Work to the Present Study

Amongst the various mathematical models developed so far to describe the atomization process the models of Bradley[1] and Lubanska[2] could be readily tested using the data obtained in the present investigations. The details of these tests are given below.

4.2.3.1 Bradley's Model

As it has already been discussed in Chapter 2, Bradley observed that the diameter of the droplet formed due to disintegration of a liquid stresm could be given as

$$d = \frac{11.8 \in}{\varphi_{max}} \qquad (4.2)$$

where φ_{max} was given by

$$\varphi_{max} = \frac{L \rho_g U_s^2}{\sigma} \qquad (4.3)$$

Substitution of Eq. (4.3) in (4.2) resulted in

$$d = \frac{11.8 \sigma \in}{L \rho_g U_s^2} \qquad (4.4)$$

TABLE 4.15

Variation of Mean Size of Powder with Variation in Operating Conditions.

Material	Temperature in °C	Atomizing angle	Nozzle dia. = 0.236 cm Average size in microns	Nozzle dia. = 0.183 cm Average size in microns	Nozzle dia. = 0.1295 cm Average size in microns
Tin	285	25°	182.6	180.7	178.4
	315	15°	198.0	188.4	193.1
		25°	175.8	175.1	169.7
		35°	174.3	156.9	120.0
		45°	133.7	-	-
	375	25°	172.0	171.1	166.2
Lead	375	15°	196.5	187.3	191.4
		25°	172.0	168.0	164.9
		35°	172.3	154.6	114.7
Lead-Tin alloy	285	25°	181.1	171.4	169.5
	315	25°	177.2	167.3	165.1
	345	25°	168.8	171.2	160.1
	375	25°	163.3	159.2	160.0

Bradley arbitrarily took $\epsilon = 1/4$ to modify the above equation as

$$d = \frac{2.95\,\gamma}{L\,\rho_g\,U_s^2} \qquad (4.5)$$

The value of the parameter L was found from a universal graph[1] of L vs Mach number.

To test the validity of this model for our data, Mach number of the impinging gas was calculated (horizontal component of velocity was used to calculate the Mach number) and the value of L was obtained from the universal curve of L vs M, given by Bradley[1]. The value of the average drop diameter was then obtained using Eq. (4.5). The values of mean sizes of powders obtained under various conditions of atomization and the values of various parameters used for evaluating these mean sizes are given in Table 4.16. The values of experimentally observed mean sizes are also tabulated along with theoretically predicted mean sizes in this table. The large discrepancies between the theoretically predicted and experimental values are obvious and can be attributed to the fact that there is no justification in assuming a constant value of ϵ in a priori. In general, ϵ should depend on operating conditions and the design parameters. To illustrate this fact, a simple linear relation of the type

$$\epsilon = \bar{A} + \bar{B}\,\theta + \bar{C}\,D \qquad (4.6)$$

TABLE 4.16

Comparison of the Theoretically Predicted Mean Sizes Using Modified Bradley's Model with that of Predicted by Using Bradley's Model, and the Experimental Mean Sizes

Nozzle dia. in cms.	Material	Atomizing angle θ	L from universal curve	$\bar{d}_m^{x}$ in mm	$\bar{d}_m^{xx}$ in mm	ϵ^{*}	ϵ^{**}	$\bar{d}_m^{xxx}$ in mm	$\sum(\bar{d}_m^{xx} - \bar{d}_m^{xxx})^2$
0.236	Tin	15^o	0.025	0.49	0.20	0.1009	0.1236	0.24	1.7×10^{-3}
		25^o	0.060	0.20	0.18	0.2150	0.2236	0.18	
		35^o	0.100	0.12	0.17	0.3551	0.3237	0.16	
	Lead	15^o	0.025	0.41	0.20	0.1195	0.1477	0.24	1.8×10^{-3}
		25^o	0.060	0.17	0.17	0.2510	0.2631	0.18	
		35^o	0.100	0.10	0.17	0.4190	0.3786	0.16	
0.183	Tin	15^o	0.025	0.49	0.19	0.0960	0.1036	0.20	0.3×10^{-3}
		25^o	0.060	0.20	0.18	0.2142	0.2037	0.17	
		35^o	0.100	0.12	0.16	0.3197	0.3038	0.15	
	Lead	15^o	0.025	0.41	0.19	0.1139	0.1222	0.20	0.2×10^{-3}
		25^o	0.060	0.17	0.17	0.2452	0.2377	0.16	
		35^o	0.100	0.10	0.15	0.3760	0.3532	0.15	
0.1295	Tin	15^o	0.025	0.49	0.19	0.0984	0.0835	0.16	1.7×10^{-3}
		25^o	0.060	0.20	0.17	0.2076	0.1836	0.15	
		35^o	0.100	0.12	0.12	0.2445	0.2836	0.14	
	Lead	15^o	0.025	0.41	0.19	0.1164	0.0965	0.16	1.4×10^{-3}
		25^o	0.060	0.17	0.16	0.2407	0.2120	0.15	
		35^o	0.100	0.10	0.11	0.2789	0.3275	0.13	

ϵ^{*} is the value obtained using Bradley's equation (Eq. 4.4)

ϵ_x^{**} is the value obtained using Eqs. (4.7) or (4.8)

$\bar{d}_m^{xx}$ is the value of mean size predicted by Eq. (4.5)

$\bar{d}_m$ is the experimental value of mean size

$\bar{d}_m^{xxx}$ is the value of mean size evaluated by using ϵ^{**} in Eq. (4.4)

was assumed. Regression analysis was carried out to evaluate the values of constants $\bar{A}$, $\bar{B}$, $\bar{C}$ in the above equation using six experimental points. The six experimental points used for regression analysis, in the case of tin, were the points obtained at 315 °C for two nozzles of different diameters, namely, 0.236 cm and 0.1295 cm, using three different atomizing angles. In the case of lead, only the operating temperature was different and it was 375 °C. Using Eq. (4.4) and the experimental values of mean particle size the values of ϵ were obtained (Table 4.16) and these values were then used in the regression analysis. The following linear regression equations were obtained for tin and lead, respectively

$$\epsilon = -0.11534 + 0.57334\,\theta + 0.37624\,D \qquad (4.7)$$

and

$$\epsilon = -0.13886 + 0.66163\,\theta + 0.48016\,D \qquad (4.8)$$

Using the above equations the ϵ values for a nozzle of 0.183 cm diameter and three different atomizers were obtained for both tin and lead, and these ϵ values were then used to predict the mean size using Eq. (4.4). Theoretically predicted values of mean particle size using Eq. (4.4) and Eqs. (4.7) and (4.8) for tin and lead respectively are tabulated in Table 4.16. The comparison between the experimental and theoretically predicted values

of mean powder size is presented in the form of sum of the squares of the residuals. From the Table 4.16 it is obvious that this value for 0.183 cm nozzle is smaller than that for 0.236 cm and 0.1295 cm nozzle, which were used for regression analysis. It should, however, be recognized that to obtain a more rigorous and perhaps a general equation for ϵ , one will need many more data points. The main objective here is to show that the discrepancies, between the experimental values of mean particle size and that of theoretical predicted values using Eq. (4.5), can be reduced to a very large extent by using a more general expression for ϵ . It is even possible to use higher order equations for ϵ , provided one has larger number of data points.

4.2.3.2 Lubanska's Model

Modifying Wigg's formula[12] to satisfy his experimental data, Lubanska[2] proposed the following correlation

$$\frac{\bar{d}_m}{D} = K_1 \left[\left(1 + \frac{M_l}{M_g}\right) \frac{\nu_l}{\nu_g We} \right]^{1/2} \qquad (4.9)$$

Using a constant value for K_1 (50), he observed that all his experimental data points obtained under various conditions of atomization for various metals, when plotted as $\left(1 + \frac{M_l}{M_g}\right) \frac{\nu_l}{\nu_g We}$ vs $\frac{d_m}{D}$ on a log x log

paper, fell on a straight line. The value of the exponent obtained from the slope of this line was found to be 1/2.

The experimental data obtained in this investigation, however, failed to satisfy the above correlation. The correlation was therefore modified and is given below

$$\frac{\bar{d}_m}{D} = K_D \left[\left(1 + \frac{M_l}{M_g}\right) \frac{\nu_l}{\nu_g \, We} \right]^{m_\theta} \qquad (4.10)$$

The proposed correlation differs from Lubanska's correlation in two respects, namely, the constant K_D and the exponent m_θ in Eq. (4.10) are no longer constants and may have different values for different operating conditions. As it will be shown later on, the parameter K_D is strongly dependent on nozzle diameter, and the exponent m_θ is a function of design of the atomizer but independent of nozzle diameter.

Figure 4.11 is a plot of $\log \left[\left(1 + \frac{M_l}{M_g}\right) \frac{\nu_l}{\nu_g \, We} \right]$ vs $\log \left(\frac{\bar{d}_m}{D} \right)$ for tin, lead, and lead-tin alloy at various temperatures for three different nozzles, namely, 0.236 cm, 0.183 cm, and 0.1295 cm diameters, respectively. The atomizing angle for all these experimental points is 25°. From the figure it is evident that the data points for various metals obtained at various temperatures tend to fall on a straight line as long as the nozzle diameter is kept constant. However, the different straight lines

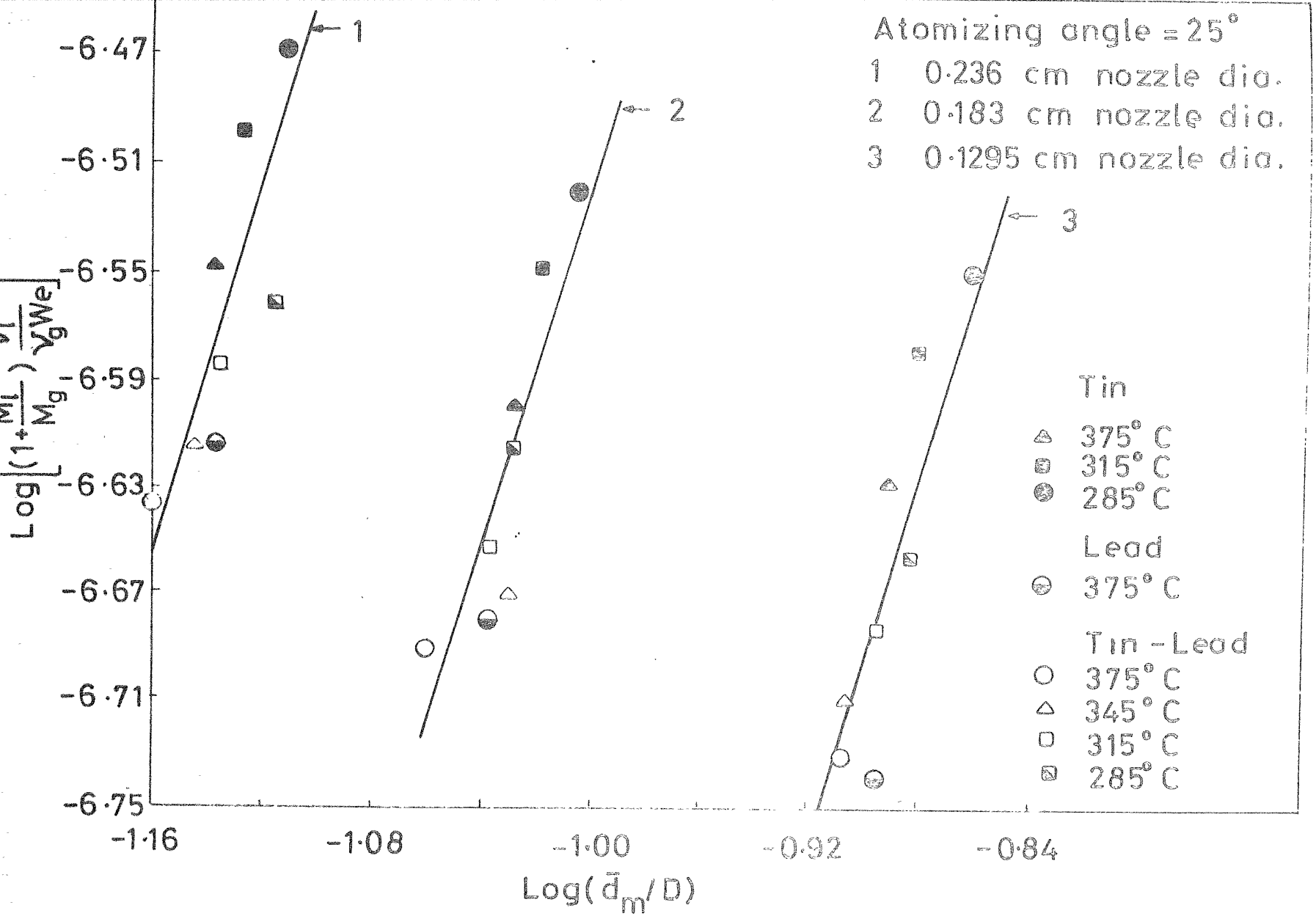

Fig. 4·11 Plot of $\text{Log}\left[(1+\frac{M_l}{M_g})\frac{\nu_l}{\nu_g We}\right]$ vs $\text{Log}(\bar{d}_m/D)$ - effect of nozzle diameter

obtained for three different nozzles clearly indicate that the parameter K_D is a strong function of nozzle diameter. It should further be noticed that the three straight lines corresponding to the three nozzles are parallel to each other indicating that the exponent m_θ in Eq. (4.10) is independent of nozzle diameter. The equation of the straight lines would be of the form

$$\log \left(\frac{\bar{d}_m}{D} \right) = \log K_D + m_\theta \log \left[\left(1 + \frac{M_l}{M_g}\right) \frac{\nu_l}{\nu_g \, We} \right] \qquad (4.11)$$

where m_θ and K_D are the slopes and intercepts of the straight lines, respectively. The slope of the lines in Fig. (4.11) was evaluated and the value of exponent was found to be 0.293. Using this value of the exponent, the values of intercepts for three different nozzle diameters were obtained and are tabulated in Table 4.17a.

The values of the various parameters used in the above correlation are given in Appendix 1.

4.2.4 Effect of Operating Variables on Atomization Process

4.2.4.1 Effect of Nozzle Diameter

The experimental data obtained using nozzles of three different opening diameters, namely, 0.236 cm, 0.183 cm, and 0.1295 cm, for tin, lead, and lead-tin eutectic alloy at different temperatures and different atomizing angles is tabulated in Tables 4.2 to 4.14.

TABLE 4.17 a

Estimated Values of the Parameter K_D for Various Nozzle Diameters.

Diameter of the nozzle in cms.	K_D
0.236	6.265
0.183	8.260
0.1295	11.670

TABLE 4.17 b

Estimated Values of the Exponent m_θ for Various Atomizing angles and nozzle diameters.

Nozzle diameter in cms. \ Atomizing angle	15°	25°	35°
0.236	0.302	0.293	0.280
0.183	0.304	0.293	0.287
0.1295	0.300	0.291	0.303
Average value of m_θ	0.302	0.293	0.284

Figures 4.1 to 4.3 are the three representative plots showing the effect of nozzle diameter on atomization of tin, lead, and lead-tine eutectic alloy, respectively, where the cumulative weight percentage retained is plotted on log-probability paper. From the figures it is evident that the size distribution tends to move towards finer mean size with decreasing nozzle diameter. Table 4.15 gives the mass median diameter of the powders produced at different atomizing conditions. Simple mass median diameter vs nozzle diameter plots are shown in Figure 4.12. In absence of large enough data no attempt has been made to propose a quantitative relationship between the mass median diameter and nozzle diameter, but qualitatively the findings of this investigation are in agreement with those of Khedkar[6] and others[16,32].

Theoretically speaking, it should be possible to predict the mean diameter of the particles using the correlation given by Eq. 4.10, once the values of the exponent m_θ and the parameter K_D are established. It has already been established above, that the exponent m_θ depends only on atomizing angle and is independent of nozzle diameter, and that the parameter K_D is a function of nozzle diameter alone. It should therefore, be possible to have atleast an emperical correlation between the parameter K_D and the nozzle diameter. Since we had only three

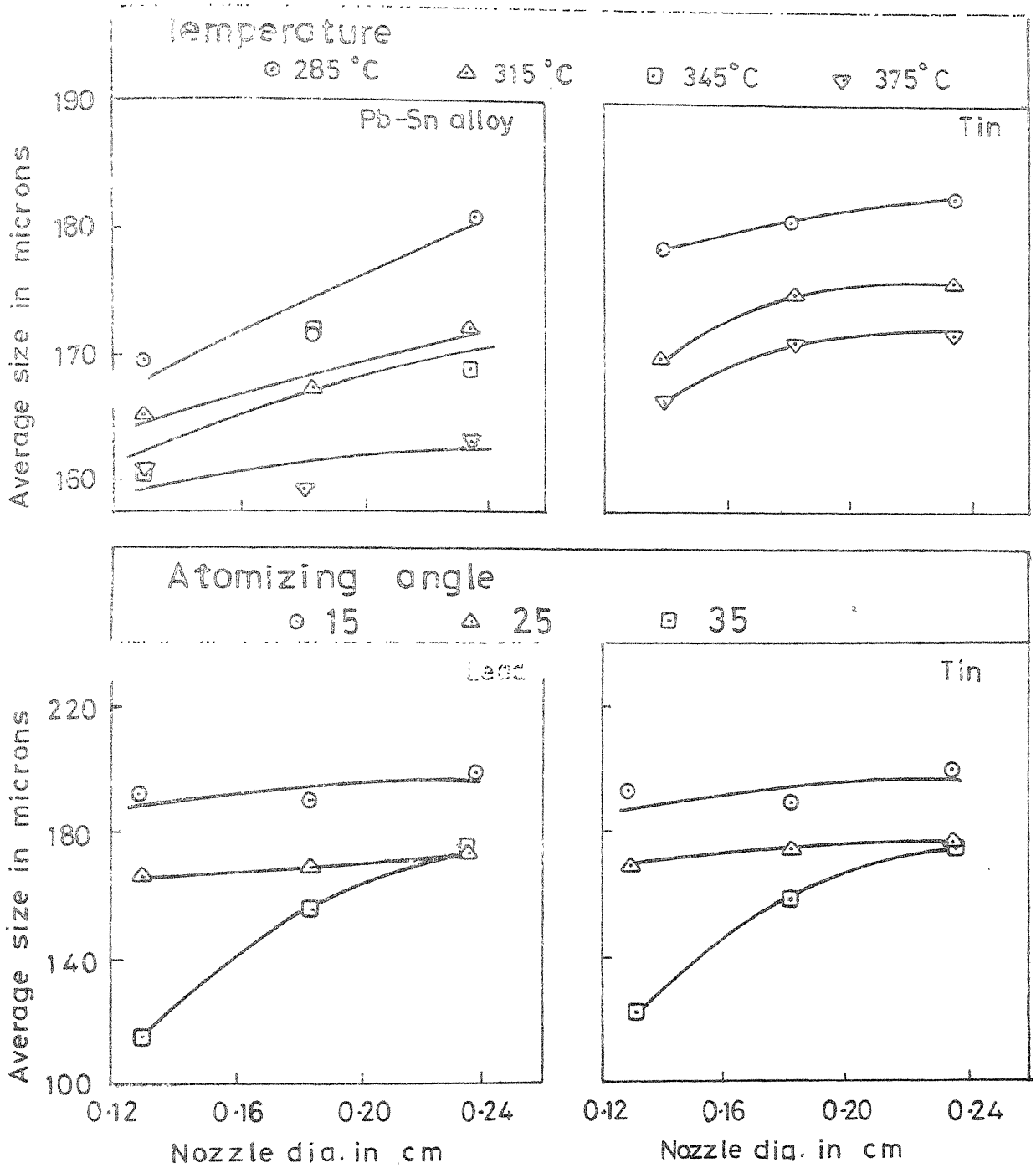

Fig. 4·12 Effect of nozzle diameter on average size

nozzles of different diameters, we had not attempted in this direction. However, a graphical correlation between the parameter K_D and the nozzle diameter is shown in Fig. 4.13. Once the K_D value is estimated for a given nozzle, either graphically or using a correlation, it would be possible to predict the mean size of the powder.

It is possible that the discrepancy between our observations and that of Lubanska who found mean size to be independent of nozzle diameter is due to the fact that in the present investigation the nozzles used were of much smaller in diameters (the biggest nozzle was 0.236 cm) as compared to the ones used by Lubanska where the diameters varied from 0.63 cm to 2.22 cm.

4.2.4.2 Effect of Atomizing Angle

The experimental data on atomization using different atomizing angles for tin and lead at various temperatures using various nozzles is tabulated in Tables 4.3 to 4.5, 4.8 to 4.10. The effect of atomizing angle on cumulative size distribution for tine and lead is shown in Figures 4.4 to 4.6. From the figures it is evident that the size distribution tends to shift towards finer mean size with increasing atomizing angle. Simple mass median diameter vs atomizing angle plots are shown in Figure 4.14.

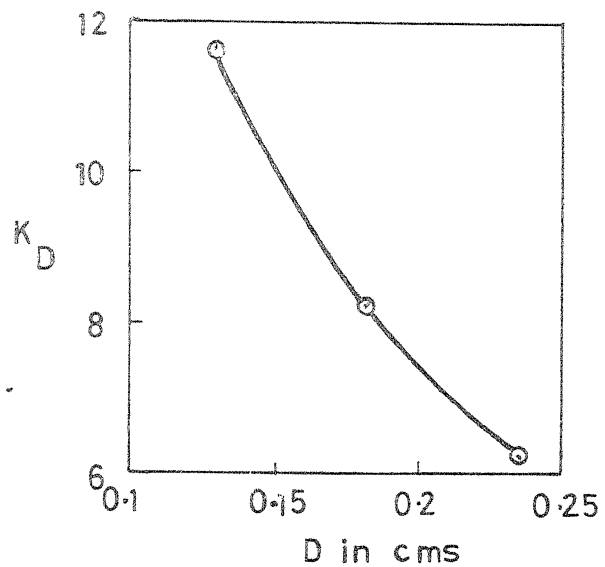

Fig. 4·13 Variation of K_D with D

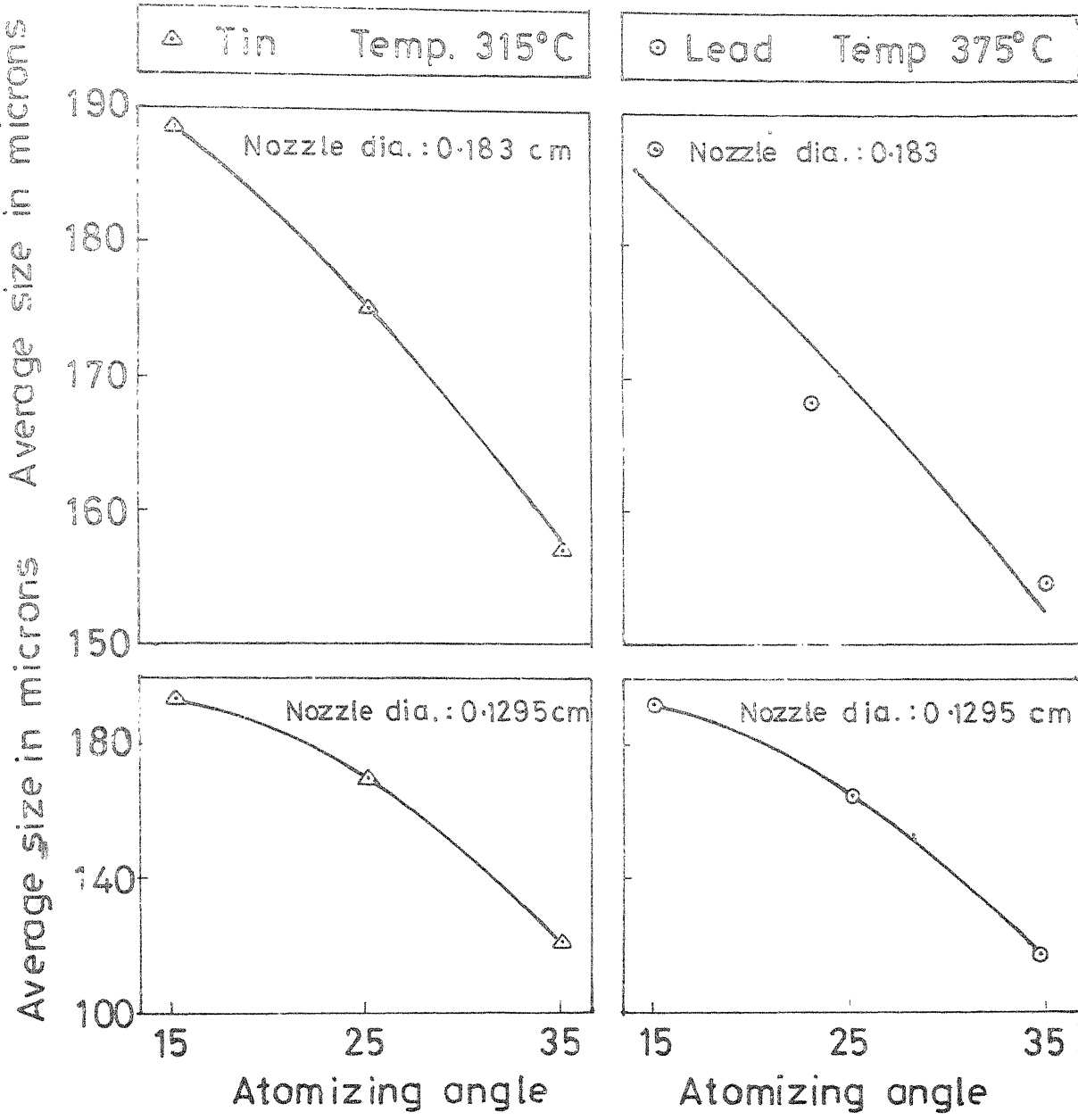

Fig. 4·14 Effect of atomizing angle on average size

It should be possible to predict the effect of atomizing angle on mean size using modified correlation. A plot of log $\left[(1 + \frac{\mu_l}{\mu_g}) \frac{\nu_l}{\nu_g We}\right]$ vs log ($\bar{d}_m/D$) showing the effect of atomizing angle on experimental data for tin, for the three nozzles, is shown in Fig. 4.15. Similar plot for lead is shown in Fig. 4.16. Using the correlation and the values of K_D, already evaluated, the values of the m_θ were obtained and are tabulated in Table 4.17b. It is evident from the table that the exponent, m_θ, remains more or less unchanged for a particular value of atomizing angle. The only exception is the point corresponding to nozzle diameter of 0.1295 cm and atomizing angle 35^o, which may be due to some error in experimental data. This point has not been used in further computations. The values of m_θ for various nozzle diameters and atomizing angles for lead were also evaluated and were found to be more or less same as for tin. It is therefore quite reasonable to assume that the exponent m_θ varies only as a function of atomizing angle. A plot of m_θ vs atomizing angle is shown in Figure 4.17. Since we had only three atomizing angles, we have not tried to proposed an emperical relation

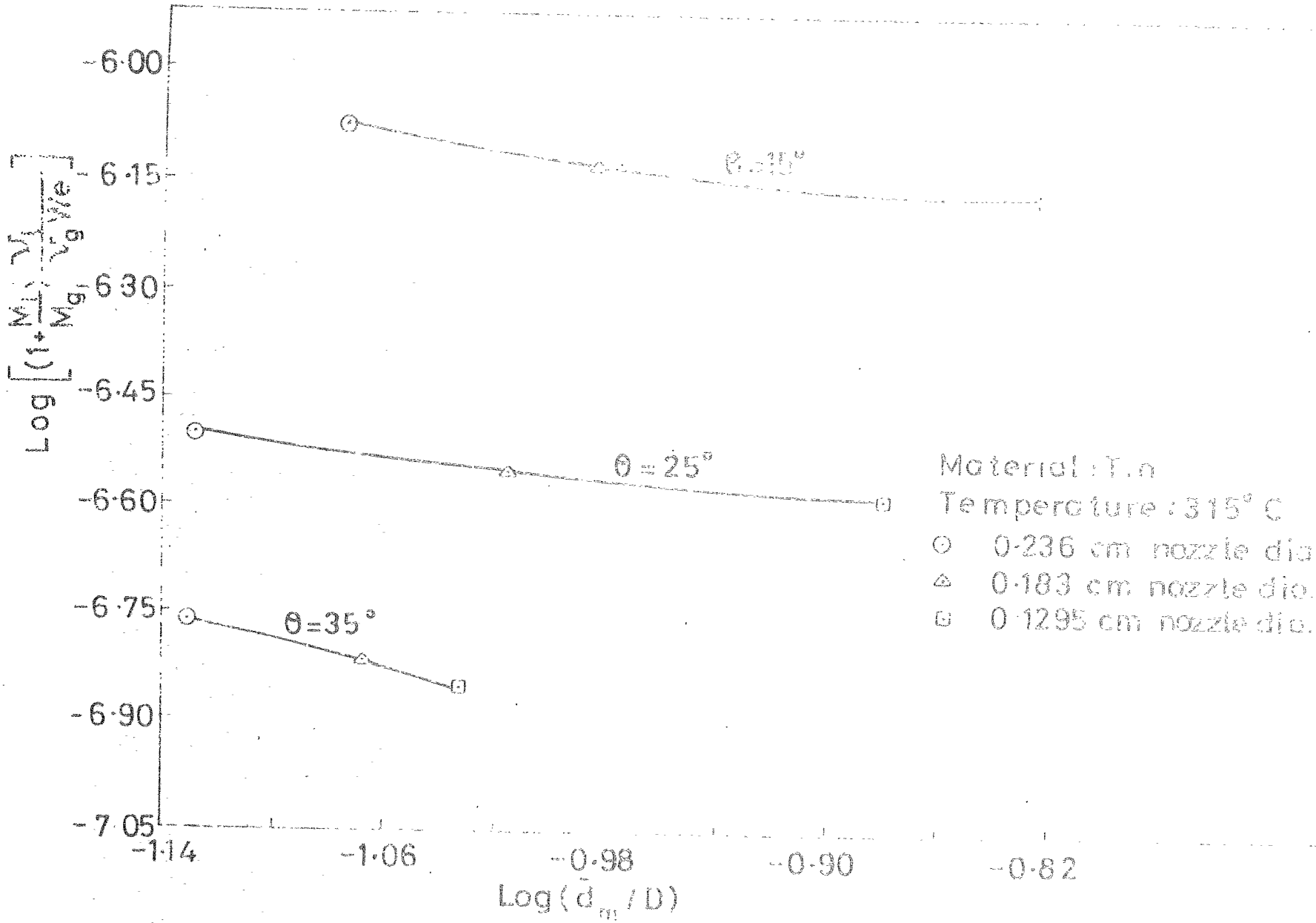

Fig. 4·15 Plot of $\text{Log}\left[\left(1+\frac{M_l}{M_g}\right)\frac{\nu_l}{\nu_g}\sqrt{We}\right]$ vs $\text{Log}(\bar{d}_m/D)$ – effect of atomizing angle

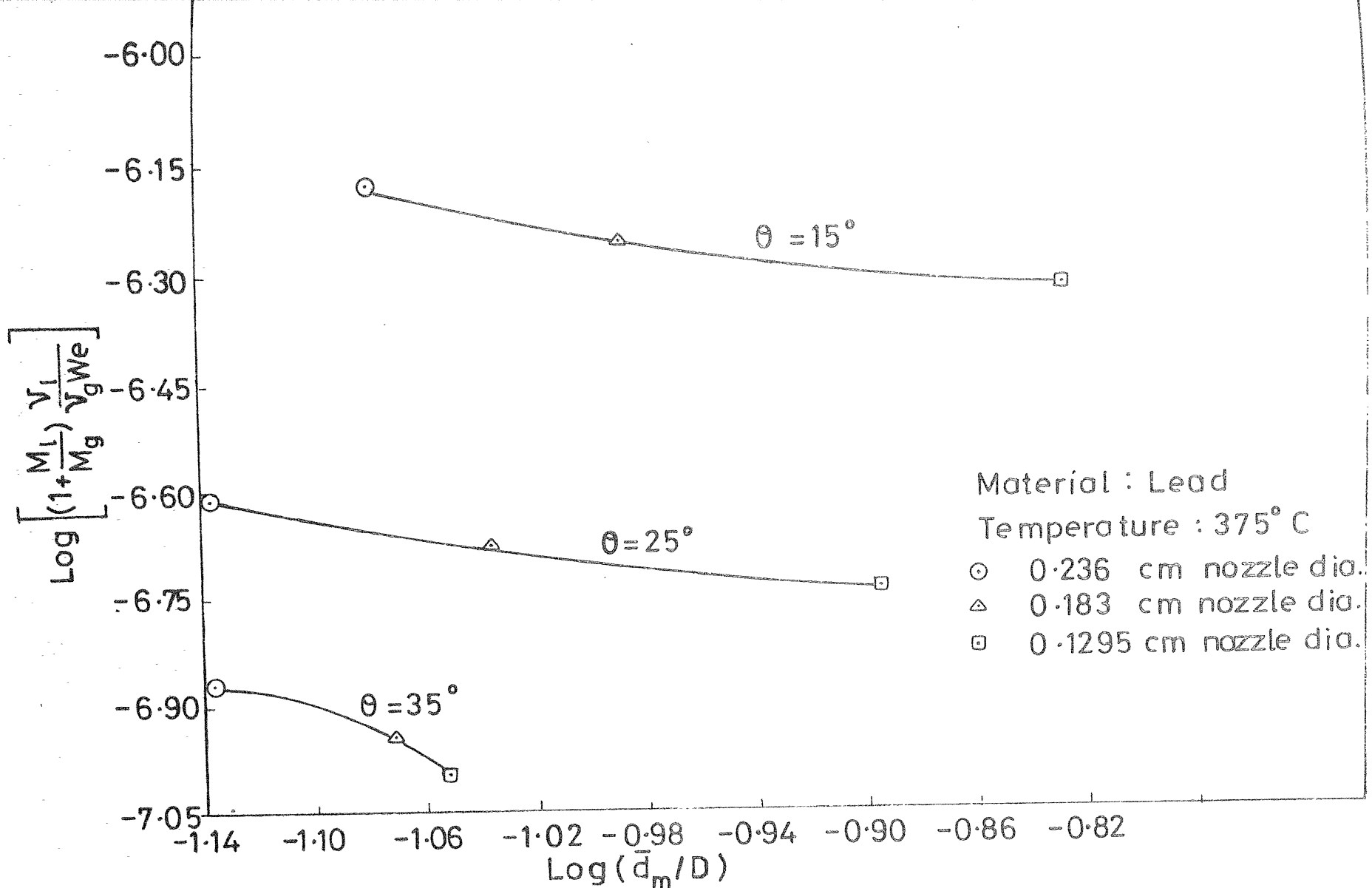

Fig. 4·16 Plot of $\text{Log}\left[(1+\frac{M_l}{M_g})\frac{\nu_l}{\nu_g We}\right]$ vs $\text{Log}(\bar{d}_m/D)$ - effect of atomizing angle

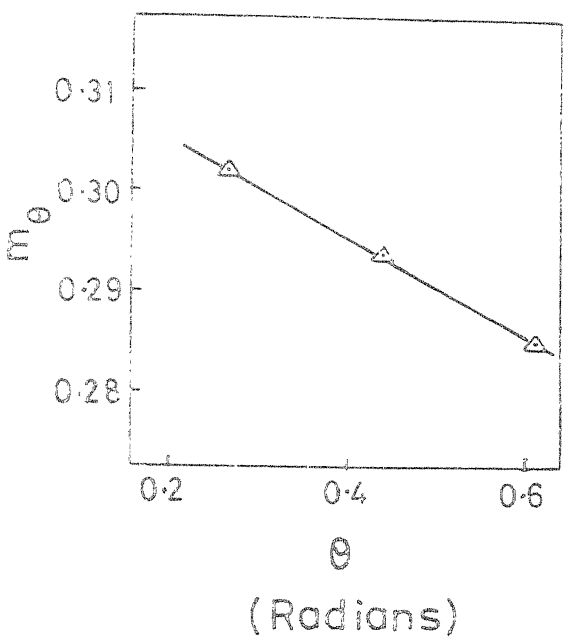

Fig.4·17 Variation of m_θ with θ

between m_θ and θ. However, once a relationship between m_θ and θ is known (either graphical or emperical), it would be possible to theoretically predict the mean size of the particles produced using atomizers of different atomizing angles.

4.2.4.3 Effect of Temperature

Experimental data showing the effect of temperature on atomization of tin and lead-tin eutectic alloy, respectively, is tabulated in Tables 4.2, 4.4, 4.7 and 4.11, 4.12, 4.13, 4.14. The plots of cumulative weight percentage retained, plotted on log-probability paper, are shown in Figures 4.7 and 4.8. It is evident from these figures that both for tin and the alloy the distribution shifts towards the finer mean size with increasing temperature. Mass median diameters of powders obtained at various temperatures for tin and the alloy are tabulated in Table 4.15. Figure 4.18 shows the variation of mean size as a function of temperature. The qualitative observation that the mean powder size decreases with increase in temperature is in conformity with that of Khedkar[6] and others.[1,2,32]

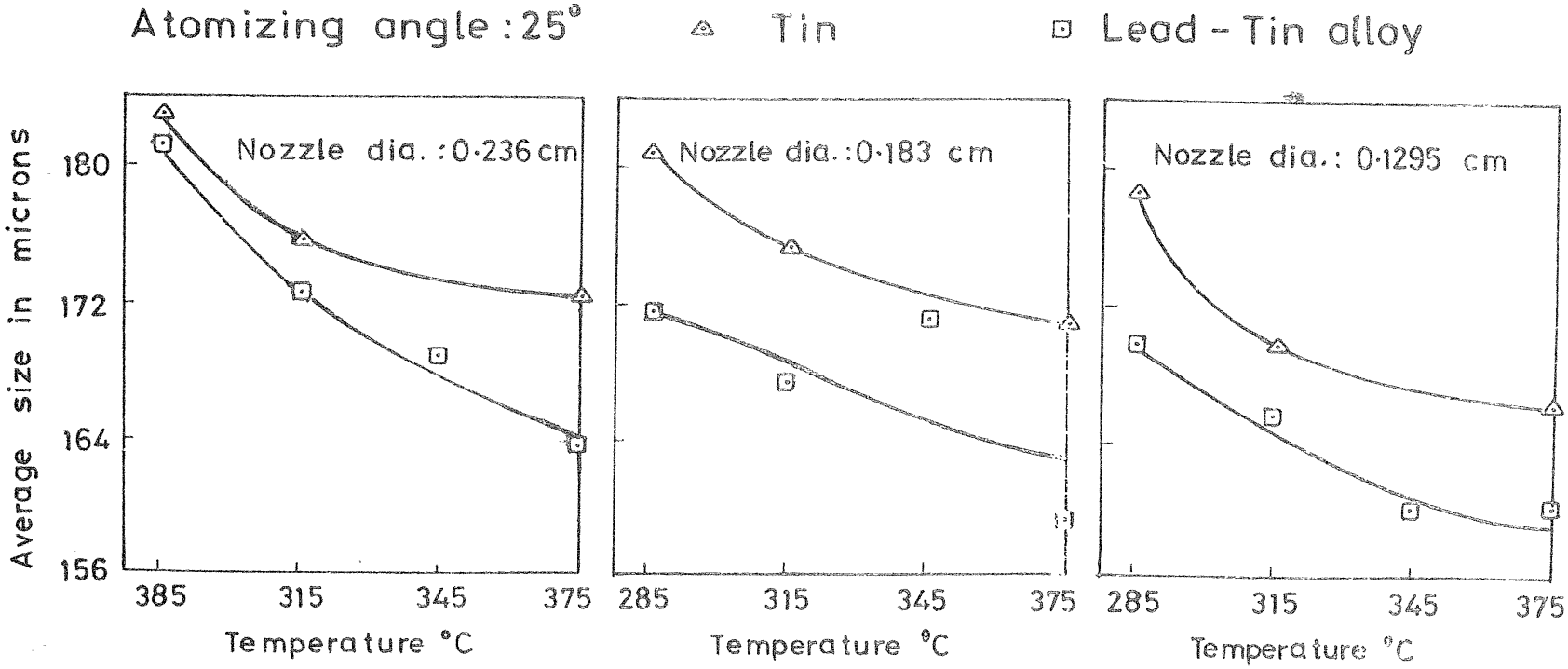

Fig.4·18 Effect of temperature on average size

It is possible to discuss the effect of temperature on mass median diameter a bit more quantitatively using the proposed correlation (Eq. 4.10). Substituting for Weber number in the correlation, we get

$$\frac{\bar{d}_m}{D} = K_D \left[\left(1 + \frac{M_l}{M_g}\right) \frac{\nu_l \sigma}{\nu_g \rho_l V^2 D} \right]^{m_\theta} \qquad (4.12)$$

In this equation the most temperature sensitive term is perhaps, the surface tension term, σ, which decreases with increase in temperature. It is, therefore, likely that the mean size will decrease with increase in temperature. A plot of $\log \left[\left(1 + \frac{M_l}{M_g}\right) \frac{\nu_l}{\nu_g We} \right]$ vs $\log \left(\frac{\bar{d}_m}{D} \right)$ showing the effect of temperature on atomization using nozzles of different diameters and atomizing angle of 25° is shown in Figure 4.19.

One remarkable feature of Figure 4.19 is that the isotherms for a given material are parallel to each other. An attempt has been made to obtain the equations for these isotherms. A parabolic equation of the form

$$y' = A' (X')^2 + B' (X') + C' \qquad (4.13)$$

was assumed, where

$$y' = \log \left[\left(1 + \frac{M_l}{M_g}\right) \frac{\nu_l}{\nu_g We} \right] \quad \text{and} \quad X' = \log (\bar{d}_m/D).$$

The values of the constants A', B', and C' were evaluated

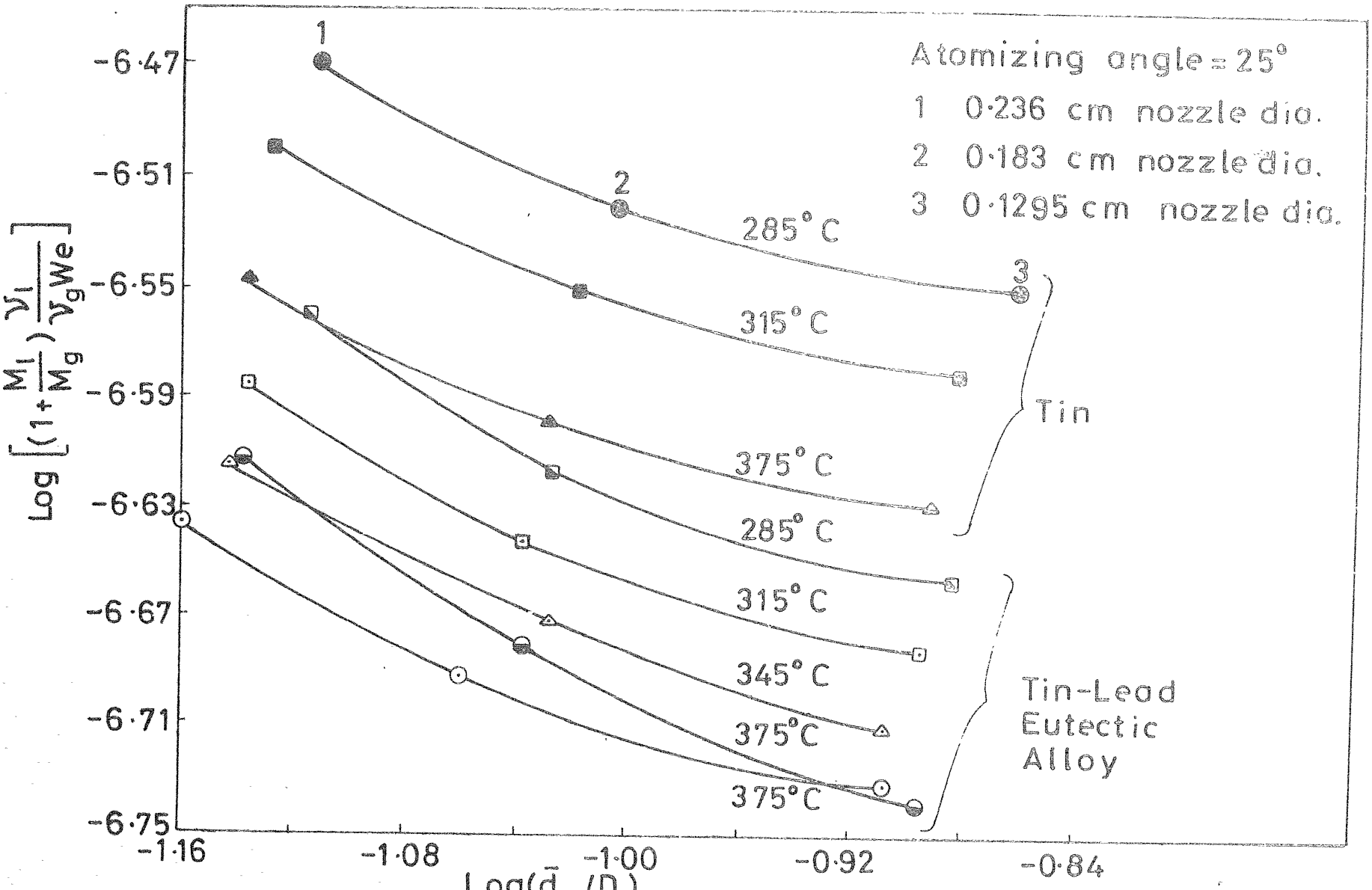

Fig. 4·19 Plot of $\text{Log}\left[\left(1+\frac{M_l}{M_g}\right)\frac{\nu_l}{\nu_g We}\right]$ vs $\text{Log}(\bar{d}_m/D)$ - effect of temperature

using the three points at a particular temperature, both for tin and alloy, respectively. The final equations obtained at 315 ^{o}C for tin was

$$y' = 1.038924\ (X')^2 + 1.7569378\ (X') - 5.455128 \qquad (4.14)$$

and for the alloy was

$$y' = 1.2828521\ (X')^2 + 2.2091139\ (X') - 5.3493981 \qquad (4.15)$$

It should be noticed that only the constant C' will change with variation in temperature. Hence to predict the effect of temperature on atomization process under different conditions (eg. nozzles of different diameters), only one experimental point at that temperature would be sufficient to find out the value of the constant, C', and therefore the complete equation of the isotherm. The validity of Eqs. (4.14) and (4.15) was established by predicting the y' values using the above equations for tin and alloy, respectively, for the data points which were not used in evaluation of the values of the constants in the above equations. The remarkable agreement between the predicted and experimental values (Table 4.18) proves the reliability of these equations.

TABLE 4.18

Comparison of Theoretically Predicted Values of y' Parameter (Eq. (4.13) with that of Experimental Values

Material	Temperature ^{o}C	Nozzle diameter in cms.	C' in Eq. (4.13)	y' using Eqs.(4.14) (4.15) with corresponding C'	Experimental value of y'
Tin	375	0.236	-5.50713	-6.16143	-6.1643
		0.183		-6.21488	-6.2155
		0.1295		-6.24772	-6.2450
	285	0.236	-5.42013	-6.08950	-6.0850
		0.183		-6.13634	-6.1365
		0.1295		-6.16267	-6.1665
Lead-tin eutectic alloy	375	0.236	-5.40540	-6.24184	-6.2527
		0.183		-6.30540	-6.3094
		0.1295		-6.35360	-6.3481
	345	0.236	-5.37940	-6.22662	-6.2314
		0.183		-6.29428	-6.2883
		0.1295		-6.32762	-6.3273
	285	0.236	-5.31740	-6.18569	-6.1759
		0.183		-6.23250	-6.2330
		0.1295		-6.26781	-6.2724

4.2.4.4 Effect of Material

Figures 4.9 and 4.10 are the cumulative weight retained plots on log-probability paper, showing the effect of material on size distribution at 375°C using an atomizer of 25° and nozzles of two different diameters, namely, 0.183 cm, and 0.1295 cm, respectively. It is evident from these plots that no clear-cut conclusion can be drawn as regards the effect of material on size distribution. Experimental points for three materials, namely, tin, lead, and the alloy seem to be scattered uniformly around a straight line. Therefore, no attempt has been made to draw three separate lines corresponding to three materials and only one straight line has been drawn.

Two of the models available in literature, namely, that of Bradley and Lubanska were tested on the experimental data obtained in the present investigation. It was found that none of these models fitted with the data in their proposed form.

Modifications have been proposed for both the models for better fitting of the experimental data.

The effects of nozzle diameter, atomizing angle, temperature have been analysed both qualitatively and quantitatively. The conclusions of the present investigation are summarized below.

CONCLUSIONS

1. The powder size distribution closely follows log-normal pattern.

2. Both Bradley's and Lubanska's models failed to fit with the data in present investigation in their proposed form.

3. In case of Bradley's model the quality of the fitting is much improved if ϵ (Eq. 4.4) is taken as a function of nozzle diameter and atomizing angle and not as a constant = 0.25 as proposed by Bradley. Following linear equations have been proposed for ϵ for tin and lead respectively:

$$\epsilon = -0.11534 + 0.57334\ \theta + 0.37624\ D$$

and

$$\epsilon = -0.13886 + 0.66163\ \theta + 0.48016\ D$$

4. In the case of Lubanska's model it has been observed that the following modified correlation gives a better fit

$$\frac{\bar{d}_m}{D} = K_D \left[\left(1 + \frac{M_l}{M_g}\right) \frac{\nu_l}{\nu_g\ We} \right]^{m_\theta}$$

This correlation differs from that of Lubanska in two respects, namely, K_D and m_θ are no longer constants. K_D is found to be a function of nozzle diameter, where as m_θ depends on atomizing angle. Graphical relationships between K_D and nozzle diameter, and m_θ and atomizing angle are shown in Fig. 4.13 and 4.17, respectively.

5. A method to predict the effects of nozzle diameter and atomizing angles on mean particle size using the modified correlation has been proposed. It has been observed that the mean size decreases with decreasing nozzle diameter and increasing atomizing angle.

6. Qualitatively, the mean size decreases with increase in temperature due to decrease in surface tension. Quantitatively the effect of temperature on mean

size has been predicted using the proposed correlation. It has been shown that the isotherms in

$$\log \left[\left(1 + \frac{M_l}{M_g}\right) \frac{\nu_l}{\nu_g \sqrt{We}} \right] \text{ vs } \log \left(\frac{\bar{d}_m}{D} \right)$$

plots for a given material are parallel to each other and closely follow a parabolic relationship. It has been further shown that once a general isotherm equation is known, only one experimental point would be sufficient to predict the mean size of particles obtained by atomization at that temperature using different operating conditions.

REFERENCES

1. D. Bradley, "On the Atomization of Liquids by High Velocity Gases," J. Phys. D, 6 (14), 1974, pp. 1724 - 36.

2. Lubanska, H., "Correlation of Spray Ring Data for Gas Atomization of Liquid Metals," J. Metals, Vol.22, No. 2, 1970, pp. 45 - 49.

3. Richard, J. Gandzol and John, A. Tallmadge, "Water Jet Atomization of Molten Steel," A I Ch E Journal, 19 (6), 1973, pp. 1149 - 1158.

4. U.R. Date, G.S. Tendolkar and M.N. Vartak, Int. J. Powder Met., 3 (2), 1967, pp. 49 - 58.

5. H. Jones, "Cooling, Freezing and Substrate Impact of Droplets Formed by Rotary Atomization," J. Appl. Phy. D, 1971, pp. 1657 - 1660.

6. Khedkar, P.Y., "Production of Metal Powder by Atomization," M.Tech. Thesis, Dept. of Met. Eng., I.I.T. Kanpur.

7. Nukiyama, S. and Tanasawa, Y., Trans. Soc. Mech. Eng., Tokyo, 4 (86), 1938, pp. 138.

8. Mugele, R.A. and Evans, H.D., "Droplet Size Distribution in Sprays," Ind. Eng. Chem., Vol. 43, 1951, pp. 1317.

9. Ohnesorge, W., Z. angew Math. Mech., Vol. 16, 1936, pp. 355.

10. A.C. Merrington and E.G. Richardson, "The Breakup of Liquid Jets," Proc. Phy. Soc., Vol. 59, 1947, pp. 1.

11. H. Clare and A. Radcliffe, "An Air Blast Atomizer for Use with Viscous Fuels," J. Inst. Fuel, Vol. 27, 1954, pp. 510.

12. Wigg, L.D., J. Inst. Fuel, Vol. 37, 1964, pp. 500.

13. Tamura, K., Takeda, T., "A Study on Production of Copper Powder Atomization," Trans. N.R.I. for Metals, Vol. 5, 1963.

14. J.S. Thompson, J. Inst. Metals, 74, 1948, pp. 101 - 32.

15. W.A. Weiss, C.H. Worsham, A R S Journal, April 1959, pp. 252 - 59.

16. James Gretzinger, W.R. Marshall Jr., A I Ch E Journal, Vol. 7, No. 2, June 1961, pp. 312 - 18.

17. Friedman, S.J., C.O. Miller, Ind. Eng. Chem., 33, 1941, pp. 885.

18. Gelperin, N.I., Egorov, I.A., Kamneva, L.A., "Dispersion of Caustic Alkali Melts During Their Discharge From Openings in the Atomizer in a Column Granulator," Khimo. Prom - St (Moscow), (7), 1975, pp. 529 - 31 (Russ).

19. Rizkalla, A.A., Lefebure, A.H., "Influence of Liquid Properties on Air Blast Atomizer Spray Characteristics," J. Eng. Power, 97 (2), 1975, pp. 173 - 77.

20. Fainerman, V.B., "On the Atomization of Liquid by Pneumatic Sprayers," Zh. Prikl. Khim., 49 (3), 1976, pp. 553 - 57 (Russ).

21. Plateau, J.A.F., "Statique Experimentale et Theorique, etc.," Paris, 1873 (Cited by Rayleigh).

22. Rayleigh, Proc. Lond. Math. Soc., Vol. 10, 4, 1879.

23. R.A. Castleman. Jr., "The Mechanism of Atomization of Liquids," Bur. Stand. (U.S.) J. Res., 6, 1931, pp. 369.

24. J. Sauter, Forschungsarbeiten auf dem Gebiete des Inginiurwesems, No. 312, 1928.

25. Weber, C., Z. angew, Math. Mech. II, 1931, pp. 136, Ninth Progress Rept., Proj. MX - 833, Vol. II, Univ. of Colorado, Boulder. Col.

26. Tyler, E., Phil. Mag., 16, 1933, pp. 504.

27. Ernest Mayer, "Theory of Liquid Atomization in High Velocity Gas Streams," A R S Journal, 1961, pp. 1783 - 85.

28. N. Dombrowski, W.R. Johns, Chem. Eng. Sci., Vol. 17, 1962, pp. 291 - 305.

29. J. Bruce See, Joseph C. Runkle, Thomas, B. King, "The Disintegration of Liquid Lead Streams by Nitrogen Jets," Vol. 4, Nov. 1973, pp. 2669 - 73.

30. Holroyd, H.E., J. Franklin Inst., 215, 93, (1933).

31. Miesse, C.C., Jet Propulsion, 24, 237, (1954).

32. Rajinder Kumar and Kolas, S. Laxmiprasad, "Studies on Pneumatic Atomization," Ind. Eng. Chem. Process Design Develop., 10 (3), 1971, pp. 357 - 365.

33. Small, S.R. and T.J. Bruce, "The Comparison of Characteristics of Water and Inert Gas Atomized Powders," Int. J. Powder Met., Vol. 4, 1968, pp. 7.

34. Gummeson, P.V., "Modern Atomizing Techniques," Powder Met., 15, 67 (1972).

35. Straus, R., "The Mechanics of Formation of Liquid Droplets in Sprays," Ph.D. Thesis, London University, England (1949).

36. Fraser, R.R., P. Erisenklam, "Atomization of Liquid Sprays and Drop Size Analysis," Trans. of the Inst. of Chem. Engrs., Vol. 34, 1956, pp. 293 - 319.

37. C.J. Smithells, "Metal Reference Book," London, Butterworths, 1967.

APPENDIX - 1

Values of the various parameters and variables in Eq. (4.11) are computed as follows. The equation is

$$\log \left(\frac{\bar{d}_m}{D} \right) = \log K_D + m_\theta \log \left[\left(1 + \frac{M_l}{M_g} \right) \frac{\gamma_l}{\gamma_g} We \right]$$

$\bar{d}_m$, mass median diameter is taken from Table 4.15. D, diameter of nozzle is known.

Mass Flow Rate of Liquid (M_l):

Volume flow rate of liquid is known for different nozzles. When volume flow rate is multiplied by density, we get the mass flow rate. The density values, at corresponding temperatures, are taken from Fig. A-1 (the data is available in literature[37]). Density of alloy is calculated from the densities of tin and lead, on weight basis of these constituents in the alloy.

Mass Flow Rate of Gas (M_g):

Volume flow rate of gas was measured with the help of a flow meter. This value when multiplied by gas density gave the mass flow rate and it was kept constant for all the experiments.

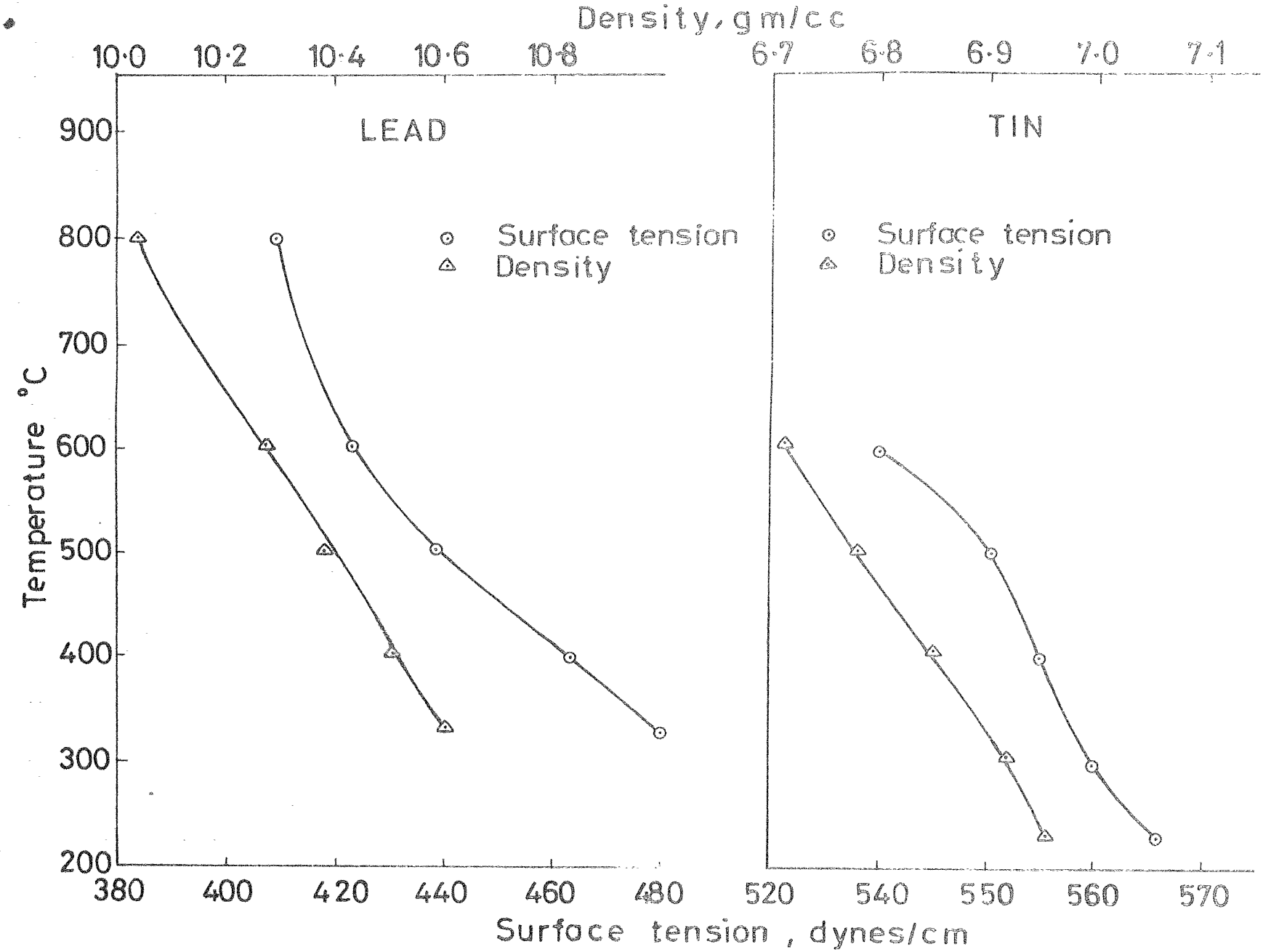

Fig. A-1 Variation of surface tension and density with temperature

Kinematic Viscosity of Liquid (ν_l):

Variation of viscosity with temperature[37], for tin and lead, is given in Fig. A-2. The absolute viscosity at any temperature is known from this graph. It is divided by density to get kinematic viscosity.

In case of alloy, superheat of the melt (temperature above its melting point) is found. Viscosities for tin and lead at that equivalent amount of superheat are evaluated. Then on weight basis of the constituents the viscosity of alloy is calculated.

Kinematic Viscosity of Gas (ν_g):

Absolute viscosity of air = 0.01861 cp

Density of air = 0.001165 g/cc

$\therefore$ Kinematic viscosity of air, $\nu_g = \frac{0.01861}{0.001165}$

$= 15.96$ cs

Calculation of Weber Number, We:

$$We = \frac{\rho_l V^2 D}{\gamma}$$

ρ_l, densities are known from the graph, for tin and lead, and for the alloy it is calculated as explained above.

V, velocity of gas is the horizontal component of velocity.

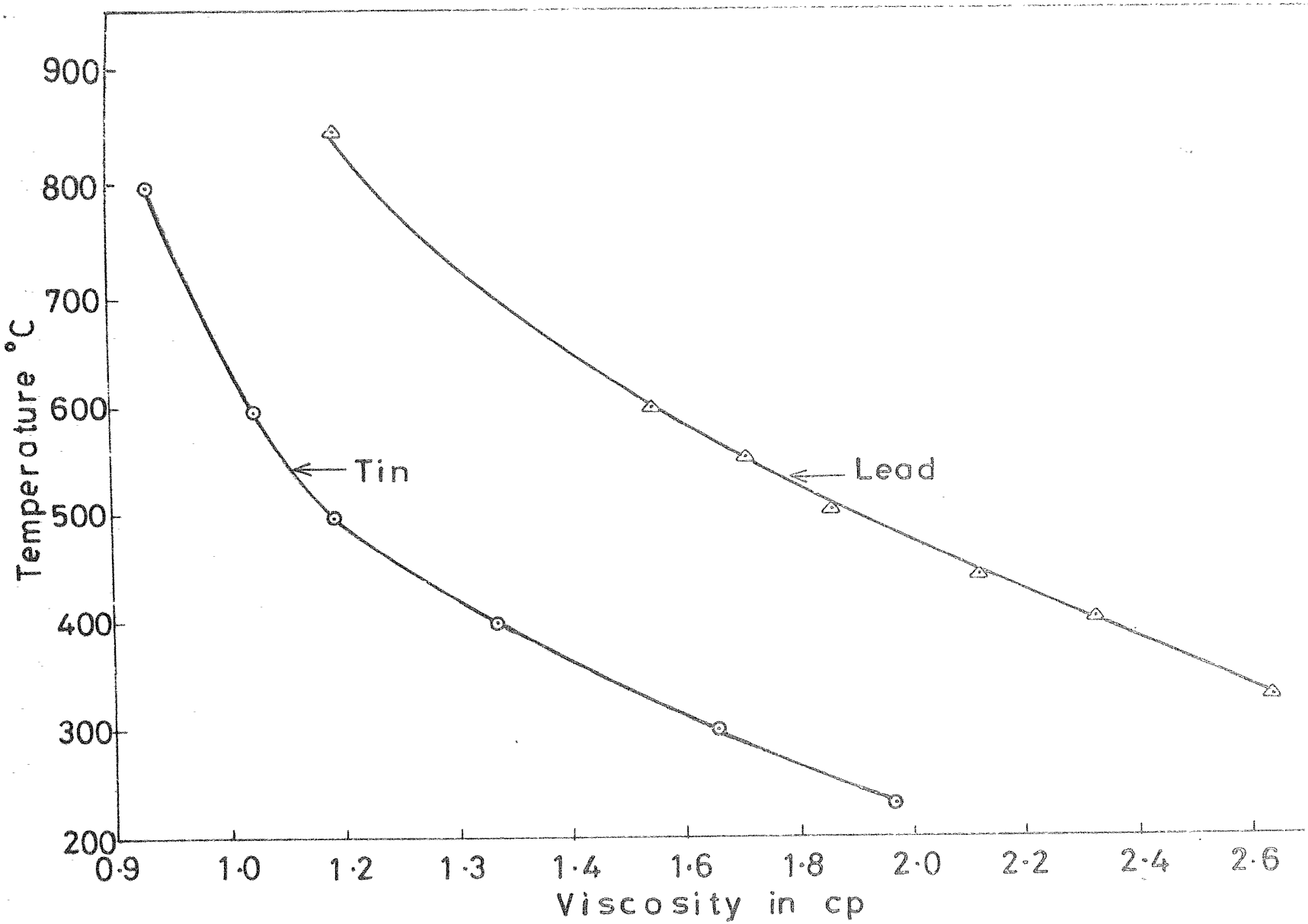

Fig. A-2 Variation of viscosity with temperature

$$\text{Air velocity, } V_a = \frac{\text{Volume flow rate}}{\text{Total area of cross section of the air jets.}}$$

$$= \frac{6100 \text{ cc/sec}}{6\,\pi\left(\frac{0.254}{2}\right)^2 \text{ cm}^2}$$

$$= 20{,}064 \text{ cm/sec}$$

$\therefore$ Velocity of gas, $V = V_a \sin\theta$

where θ is atomizing angle.

When 25° atomizer is used,

$V = 20{,}064 \times \sin 25^\circ = 8480$ cm/sec.

γ is surface tension of liquid. Variation of surface tension with temperature[37] is shown in Fig. A-1, for both tin and lead. For alloy the surface tension is calculated in a similar fashion as viscosity is calculated (explained above).

The calculated values of $\log\left[\left(1 + \frac{M_l}{M_g}\right)\frac{\nu_l}{\nu_g}\,We\right]$ and $\log\left(\frac{\bar{d}_m}{D}\right)$ at various operating conditions are tabulated in Table A-1.

TABLE A-1

Computed Values of the Parameters in Eq. (4.11)

Material	Temp. °C	Atomizing angle	Velocity of gas V (cm/sec)	D in cms	$\log(1 + \frac{M_l}{M_g})\sqrt{\rho_l/\rho_g}\,We$	$\log\left(\frac{\bar{d}_m}{D}\right)$
Lead	375	15°	5,193	0.236	-6.1883	-1.0795
				0.183	-6.2561	-0.9899
				0.1295	-6.3142	-0.8303
		25°	8,480	0.236	-6.6142	-1.1374
				0.183	-6.6820	-1.0371
				0.1295	-6.7401	-0.8950
		35°	11,508	0.236	-6.8795	-1.1366
				0.183	-6.9472	-1.0732
				0.1295	-7.0054	-1.0527
Tin	315	15°	5,193	0.236	-6.0736	-1.0762
				0.183	-6.1251	-0.9874
				0.1295	-6.1619	-0.8265
		25°	8,480	0.236	-6.4995	-1.1279
				0.183	-6.5510	-1.0192
				0.1295	-6.5808	-0.8826
		35°	11.508	0.236	-6.7647	-1.1316
				0.183	-6.8163	-1.0668
				0.1295	-6.846=	-1.0331
	285	25°	8480	0.236	-6.4693	-1.1114
				0.183	-6.5208	-1.0055
				0.1295	-6.5509	-0.8612
	375			0.236	-6.5487	-1.1374
				0.183	-6.5998	-1.0292
				0.1295	-6.6293	-0.8916
Lead-Tin Alloy	285	25°	8480	0.236	-6.5603	-1.1150
				0.183	-6.6174	-1.0284
				0.1295	-6.6568	-0.8831
	315			0.236	-6.5872	-1.1369
				0.183	-6.6442	-1.0390
				0.1295	-6.6834	-0.8945
	345			0.236	-6.6158	-1.1455
				0.183	-6.6727	-1.0289
				0.1295	-6.7116	-0.9074
	375			0.236	-6.6370	-1.1599
				0.183	-6.6938	-1.0605
				0.1295	-6.7325	-0.9081

Date Slip

This book is to be returned on the date last stamped.

CD 6.72.9